applied sciences

IMPACT FACTOR 2.5

CITESCORE 5.3

Review

Recent Progress in Multiplexed Single-Photon Sources

Peter Adam and Matyas Mechler

Special Issue

Advances in Photonics and Optics: Materials and Structures for Emerging Applications

Edited by

Dr. Giovanni Magno, Dr. Marco Grande and Dr. Ilaria Marasco

MDPI

https://doi.org/10.3390/app142311249

applied sciences

MDPI

Review

Recent Progress in Multiplexed Single-Photon Sources

Peter Adam [1,2,*,†] and Matyas Mechler [1,2,†]

[1] Institute for Solid State Physics and Optics, HUN-REN Wigner Research Centre for Physics, P.O. Box 49, H-1525 Budapest, Hungary; mechler.matyas@wigner.hun-ren.hu
[2] Institute of Physics, University of Pécs, Ifjúság útja 6, H-7624 Pécs, Hungary
* Correspondence: adam.peter@wigner.hun-ren.hu
† These authors contributed equally to this work.

Abstract: We review the progress in multiplexed single-photon sources, including overviews on heralded single-photon sources and photon-number-resolving detectors, the various approaches to multiplexing, and their successful experimental realizations. We also summarize the recent results on the theoretical description and optimization of multiplexed single-photon sources, focusing on the procedures and methods that enable the improvement of the performance of these sources.

Keywords: heralded single-photon sources; multiplexed single-photon sources; spatial multiplexing; temporal multiplexing; spectral multiplexing

Citation: Adam, P.; Mechler, M. Recent Progress in Multiplexed Single-Photon Sources. *Appl. Sci.* **2024**, *14*, 11249. https://doi.org/10.3390/app142311249

Academic Editors: Giovanni Magno, Marco Grande and Ilaria Marasco

Received: 4 September 2024
Revised: 19 November 2024
Accepted: 29 November 2024
Published: 2 December 2024

1. Introduction

Single-photon sources are fundamental elements in various experiments and numerous applications in the fields of quantum information processing and photonic quantum technology [1–6]. An ideal single-photon source can produce highly indistinguishable single photons with known polarization in near-perfect spatial modes in a deterministic way. Promising candidates for realizing such a perfect source are multiplexed single-photon sources [7–11]. The building elements of such sources are heralded single-photon sources [12–36] that rely on some nonlinear optical processes, such as spontaneous parametric down-conversion or four-wave mixing, in which photon pairs are generated. The detection of one member of a pair announces the presence of its twin photon that yields the output of the heralded source. Though heralded single-photon sources are capable of generating indistinguishable photons in near-perfect spatial modes, the probabilistic nature of the underlying processes poses a limitation on the probability of obtaining exactly one photon at the output in a given period of operation, and there is always a finite probability of obtaining more than one photon from the source. Unfortunately, the reduction of this multiphoton contribution by reducing the average number of the photon pairs generated in the nonlinear processes also leads to a reduction in the single-photon probability and increases the probability of obtaining no photons at the output. Multiplexing several low-probability heralded single-photon sources provides a solution to overcome this problem by increasing the probability of successful heralding.

Since the first proposals of multiplexed single-photon sources approximately two decades ago, numerous multiplexing schemes have been proposed and analyzed theoretically [37–57]. Also, several experimental research projects have been performed that proved the feasibility and the advantages of such sources [58–72].

In this paper, we give an overview of the recent progress in multiplexed single-photon sources. As the basic building blocks of such sources are heralded single-photon sources, in Section 2, we summarize their basic characteristics. Heralding involves photon detection; therefore, this section contains an overview of photon-number-resolving detectors, which improve the performance of these sources. In Section 3, we expound on the operation principles of multiplexed single-photon sources, and we summarize the various multiplexing

schemes proposed for realizing different types of multiplexing such as spatial, temporal, and spectral multiplexing. Next, in Section 4, we present the general theory capable of treating single-photon sources based on any type of multiplexer. Then, in Section 5, we present those theoretical results that are relevant from the point of future multiplexed single-photon source experiments and the practical realization of such sources. At the end of this section, we also give a summary of the successful experiments in which single-photon sources based on some kind of multiplexing were realized. Finally, we summarize the main points of the review and discuss the prospects of multiplexed single-photon sources.

2. Heralded Single-Photon Sources

A heralded single-photon source (heralded SPS) is composed of a source of photon pairs based on some nonlinear processes such as spontaneous parametric down-conversion [12–14,16–24,26,27,29,33–35,73–76] or spontaneous four-wave mixing [15,25,28,30–32,36], and a heralding detector. The twin photons generated in the process are termed idler and signal. The presence of the signal photon is heralded by the detection of the idler photon; hence, they are also called heralded and heralding photons, respectively. Note that most applications require the periodicity of the SPS. This can be ensured by applying pulsed pumping of the photon pair source.

Photon pair generation is an inherently probabilistic process; hence, the possible values of the number of generated photon pairs can be described by a probability distribution. In the case of multimode nonlinear processes having weaker spectral filtering, a Poissonian distribution can be assumed. For single-mode processes characterized by stronger filtering, the distribution describing the number of photon pairs is thermal [59,64,77–81]. In the latter case, the heralded SPS can yield almost identical single photons required in various experiments and applications. Assuming that the mean number of generated photon pairs is $\lambda = 1$, in the case of thermal distribution, the probability of having one generated photon pair is $P_1 = 0.25$, while for a Poissonian distribution, this probability is $P_1 \approx 0.367$. These are the highest probabilities of having a single-photon pair from a photon pair generation process. Hence, even applying an ideal detector for heralding, it is not possible to obtain higher single-photon probabilities than these values from a heralded SPS [82]. Note that the single-photon probability, that is, the single-photon yield per pump pulse (i.e., at a clock cycle), is generally termed as brightness for SPSs [9]. Another quantity characterizing the performance of heralded SPSs is the heralded fidelity F_h, which is the fidelity of the heralded photon to the one-photon state $|1\rangle$ [9,82]. The multiphoton components of the output of the heralded SPS can also be quantified by the normalized second-order correlation $g^{(2)}(0)$. Applying photon-number-resolving detectors for heralding can reduce the multiphoton noise, that is, it can increase the fidelity of the heralded photons compared to the case when a single-click (that is, threshold) detector is applied [14,22,34,35,82].

One possible realization of photon-number-resolving detectors is based on the use of click detectors in combination with either a temporal or spatial multiplexing scheme [83–97]. The performance and limitations of such schemes in the presence of various deficiencies and losses have been studied in Refs. [90,92,93,95,96]. Note that superconducting nanowire detectors widely used in quantum optical experiments are generally single-click ones without photon number resolution. However, the multi-pixel ones show this capability [98,99]. Spatial multiplexing of multiple nanowires can also result in a photon-number-resolving capability [100–105]. Superconducting nanowire detectors are noted for their high quantum efficiency, excellent timing resolution, low dark counts, and sensitivity across a broad spectral range. A lot of effort has also been paid to develop high-efficiency inherent photon-number-resolving detectors. The best known realizations of such devices are fast-gated avalanche photodiodes [106,107], quantum dot field-effect transistors [108,109], superconducting nanowire detectors [110,111], and transition edge sensors [111–121]. Transition edge sensors in the near-infrared regime have been reported to yield detector efficiencies as high as 98% [118,119] along with near-perfect photon-number discrimination in the case of

low numbers of arriving photons. An additional benefit of transition edge sensors is that they have a negligibly small dark count rate [112–114,117,121].

3. Multiplexed Single-Photon Sources

As we have described in Section 2, in heralded SPSs, the generation of single-photon pairs in the nonlinear process is accompanied by a finite probability of obtaining more than one photon pair. In addition to using photon-number-resolving detectors for heralding, another way to decrease multiphoton contribution in the heralded signals is to decrease the mean number of the generated photon pairs in the heralded source. Unfortunately, this solution reduces the output single-photon probability, too. This undesired reduction can be compensated by the multiplexing of several heralded sources, and thus, the whole multiplexed system can still be characterized by a high probability of successful heralding, eventually resulting in a higher single-photon probability at the output of the multiplexed SPS. Multiplexing involves routing the signals originating from the particular heralded sources realized in space, time, or in different spectral modes to a single-output mode by using a switching device. Corresponding to the various realizations of the sources of the heralded photons to be multiplexed, spatial, temporal, and spectral multiplexing have been developed in the literature. In the following, we review each of these types of multiplexing.

3.1. Spatial Multiplexing

The idea of spatial multiplexing proposed first in Ref. [38] relies on the parallel use of a number of pulsed heralded SPSs. Photon pairs needed in the individual heralded sources can be created in separate nonlinear processes or in physically separate spatial modes of a single-photon pair source. Following the successful heralding of a heralding photon in one of the heralded sources, a spatial multiplexer, that is, an $N \times 1$ switch, routes the twin of the photon to a single output.

Such a switch can be realized by using binary photon routers. A binary photon router is actually a 2×2 switch, that is, it has two input and two output ports. One of the output ports is used as the actual output of the router, while the other output port, the so-called noise port of the router, is used to remove unnecessary photons from the multiplexer. Photons arriving at any of the input ports of the router experience losses while propagating from the input port to the output port of the router. The losses assigned to the two input ports of the router are described by transmission coefficients denoted by V_r and V_t, as were introduced in Refs. [48,53]. In general, $V_r \neq V_t$, meaning the routers are asymmetric. There are various types of optical switching devices that can act as photon routers. In multiplexed single-photon experiments, bulk electro-optic polarization rotating switches [37,39,58,62,64], integrated opto-ceramic switches [59,60,67] or electro-optic switches [61,65] were applied.

Photon routers can be used to build binary tree spatial multiplexers with various structures. The operation of the multiplexer is governed by a control unit, the operation of which is triggered by the heralding detectors. To guarantee the time needed to realize the switching, the signal photons are generally retarded by delay lines to delay their arrival to the input of the multiplexer. To facilitate the unified discussion of multiplexed SPSs, it is useful to apply the concept of multiplexed units comprising a source of heralded photons and an optional delay line. In the case of multiple heralding events in different multiplexed units, the control unit decides which heralded photons are to be forwarded to the output.

Though the structure of the multiplexer can be arbitrary, special attention has been given to certain systematic building logics. The following terms can be used for describing a multiplexer. The arms of the multiplexer are formed by the connections between the photon routers. A branch is a subtree of the multiplexer. A level of a multiplexer is formed by photon routers at an equal distance from the output of the multiplexer. As real multiplexers always have losses, a photon entering the multiplexer vanishes with a certain probability. The losses of the arms of the multiplexer can be described by transmission coefficients denoted by V_n. Note that in the case of multiple detection events in different multiplexed

units, the control unit should choose the arm with the smallest loss, that is, with the highest transmission coefficient V_n.

One type of spatial multiplexer is called symmetric, log-tree, or complete binary-tree multiplexer. Such a multiplexer is characterized by a power-of-two number of inputs (that is equal to the number of multiplexed units) and photon routers arranged so that all the levels of the binary tree are complete. Such multiplexers are discussed in Refs. [58,59,61,63,64]. The formula describing the transmission coefficients of a symmetric multiplexer can be found in Ref. [48].

Another remarkable group of spatial multiplexers are asymmetric multiplexers [41,45,52]. Figure 1a shows the schematic figure of an SPS based on an asymmetric multiplexer. During the building of such a multiplexer, the output of the next photon router is connected to one of the inputs of the previous router; thus, the consecutive photon routers form a chain-like structure. Though the chosen input port of the previous router to which the output of the next router is connected can be arbitrary, it can be proved that to obtain higher single-photon probabilities, the input port with the smaller loss is the right choice. An important advantage of such multiplexers over symmetric multiplexers is that the number of multiplexed units in the resulting structure is not limited to power-of-two numbers. The transmission coefficients of this type of multiplexer can be written as [54]

$$V_n = \begin{cases} V_b V_{\min} V_{\max}^{n-1} & \text{if } n < N, \\ V_b V_{\max}^{n-1} & \text{if } n = N, \end{cases} \tag{1}$$

where $V_{\min} = \min(V_r, V_t)$, and $V_{\max} = \max(V_r, V_t)$.

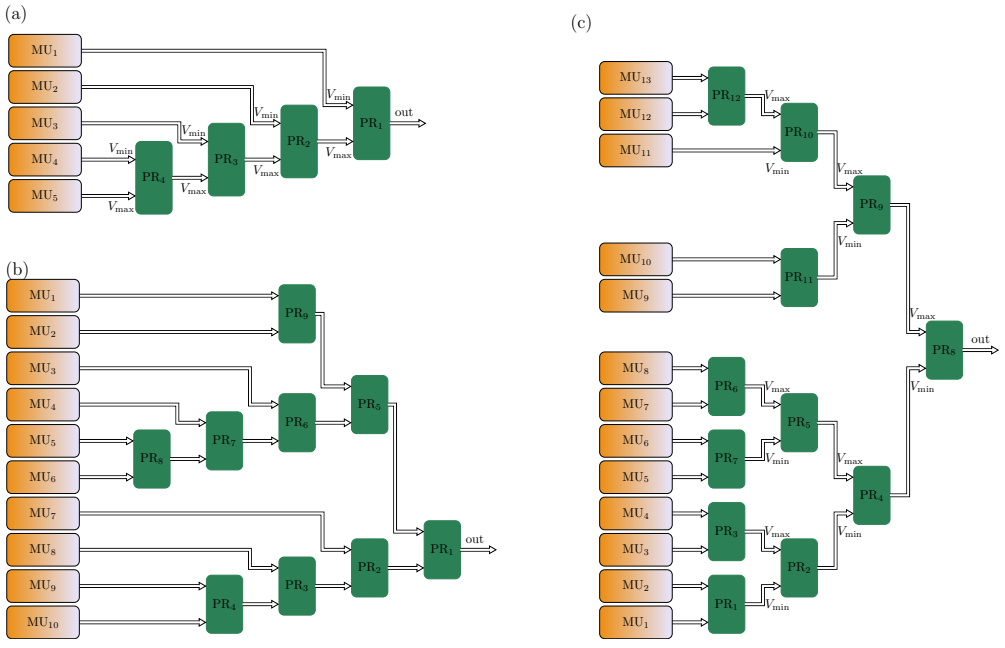

Figure 1. (**a**) Schematic figure of asymmetric multiplexer-based SPSs. (**b**) Schematic figure of an example of SOBTM-based SPSs. (**c**) Schematic figure of OMAXV multiplexer-based SPSs. MU_is are multiplexed units. PR_is are photon routers. $V_{\max}$ and $V_{\min}$ are the larger and smaller transmission coefficients, respectively, of the photon routers.

Recently, novel types of multiplexers called incomplete binary tree multiplexers were proposed [53,54]. These multiplexers are termed incomplete because, as opposed to complete binary-tree multiplexers, the levels of these multiplexers are not complete in general, although for a certain number of photon routers, these multiplexer types include symmetric multiplexers as a special case. Such multiplexers have the same advantage over symmetric

multiplexers as asymmetric multiplexers, that is, no doubling of the number of multiplexed units is required to form possible multiplexers.

Input-extended incomplete binary tree multiplexers can be assembled as follows. Let us start with a complete binary tree formed by a given number of photon routers. This multiplexer is extended by attaching the novel routers to the next level of the tree one by one from left to right (or vice versa) until the next level becomes complete. The formula describing the transmission coefficient of such multiplexers can be found in Ref. [53].

The building strategy of output-extended incomplete binary-tree multiplexers can also be explained by starting from a complete binary tree multiplexer. In this case, the output of the initial complete binary multiplexer is connected to one of the inputs of a novel photon router termed as the base router. The output of the next router is connected to the free input of the base router, thus starting the incomplete branch of the multiplexer. Subsequent routers are added one by one, always to and only to the next level in the incomplete branch of the multiplexer, until the level is completed. Various extension strategies regarding the choice of the arm to which the next router is to be added were proposed in the literature [53,54]. The most important type of these multiplexers is the one in which the initially symmetric multiplexer is attached to the input of the base router characterized by the smaller transmission coefficient $V_{\min}$ (minimum-based), and novel routers are added to the arms of the incomplete branch characterized by the largest transmission coefficient V_n (maximum-logic). It was shown that SPSs based on minimum-based, maximum logic, output-extended, incomplete binary tree multiplexers (OMAXV multiplexers) show better performance than SPSs based on any other output-extended incomplete binary tree multiplexers for a wide range of the parameters characterizing such devices [54]. Hence, in the literature, this type of spatially multiplexed SPS was analyzed and compared to other SPSs. The formula describing the transmission coefficients of SPSs based on OMAXV multiplexers has been stated in Ref. [54]. Figure 1c shows an example of the structure of an SPS based on OMAXV multiplexers.

The last type of spatial multiplexers is the stepwise-optimized binary tree multiplexer (SOBTM) [55]. In this case, the structure of the multiplexer is systematically optimized during its construction, considering the performance of the SPS where the multiplexer is applied. The position of a photon router connected to the tree in a building step can be found in consideration of the achievable single-photon probability of the source. The method chooses the position of the router for which this output probability is maximal. This building strategy is scalable, that is, one can determine the optimal multiplexer structure for any number of routers. Figure 1b shows an example of the structure of an SPS based on an SOBTM. Note that such spatial multiplexers are general binary trees, and their structure can be considerably different depending on the actual values of the router transmission coefficients. Hence, there is no general formula describing the transmission coefficients V_n of SPSs based on SOBTMs. Further examples of SPSs based on SOBTMs can be found in Ref. [55].

3.2. Temporal Multiplexing

Temporal multiplexing was first proposed and demonstrated experimentally in 2002 [37]. In this type of multiplexing, a non-deterministic photon generation process of a heralded source is repeated in time with period T. The planned time period T_S of the multiplexed source must be chosen as an integer multiple of the time period T, that is, $T_S = NT$. Within a period T_S, if the heralding event occurs at the nth time bin ($n = 1, \ldots, N$), the corresponding signal photon is delayed so that it reaches the output of the multiplexer at the end of the period T_S. Accordingly, in the case of temporal multiplexing, the temporal modes of the same heralded source are multiplexed. The signal photons potentially arriving from the heralded source during the observation time T_S can be reasonably delayed by at least T_S, which makes it possible to choose the photon from the time bin closer to the end of the predefined time period T_S. At this choice, the signal photon experiences lower loss during time multiplexing. Note, however, that the switching realized by the control unit requires

additional time; therefore, the realized time period T_R of the temporally multiplexed SPS is greater than the planned time period, that is, $T_R > T_S$. The time bins and the delay lines together play the role of multiplexed unit in the case of temporally multiplexed SPSs.

Two setups realizing temporal multiplexing were proposed in the literature. One setup utilizes storage loop (or cavity) delays [37,39,46,47,49] with a fixed delay time T. The scheme of an SPS based on such a setup is shown in Figure 2a. In this system, a heralded photon goes around the loop as many times as needed to be delayed to arrive at the end of the time period T_S. This system uses a single 2×2 switch that routes the photon into or out of the delay loop, or it simply forwards the photon to its output if no delay is needed. The various experimental realizations of this type of multiplexer are summarized in Ref. [9]. The transmission coefficient V_n assigned to the nth time bin can be written as

$$V_n = V_b V_d^{N-n} V_s^{N+1-n}, \tag{2}$$

where V_b is a general transmission coefficient, V_s denotes the loss characterizing the switch, V_d is the transmission coefficient of one-time-bin delay (that is, the propagation loss), and N is the total number of time bins.

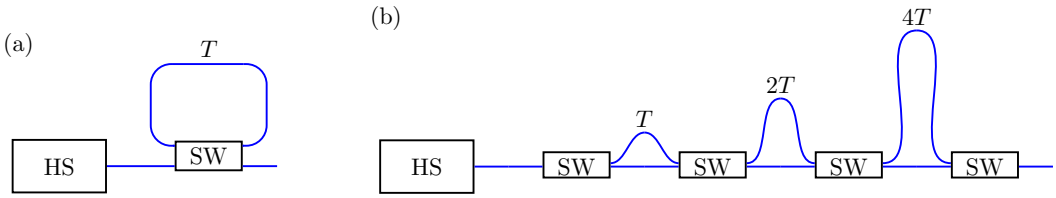

Figure 2. Schematic figures of temporally multiplexed SPSs based on (**a**) a storage loop and (**b**) binary-divided delays. HSs are heralded sources, and SWs are optical switches. The various delay times realized by the various delay lines are also indicated in the figure.

The other temporal multiplexer proposed in the literature is based on binary-divided delays [42,51]. The scheme of an SPS based on this type of multiplexer is presented in Figure 2b.

It is based on several delay lines the lengths of which are power-of-two multiples of that of a unit-length delay line that realizes the delay T. Assume that the amount of delay required for the chosen signal photon to arrive at the end of the predefined period T_S is nT. The integer multiplicative factor n can be represented by a binary number. The lowest (rightmost) digit of the binary number corresponds to the shortest delay line realizing T, while the highest (leftmost) digit belongs to the delay line realizing the longest delay. The signal photon chosen to be routed through the multiplexer is directed into those delay lines of the multiplexer for which the corresponding digit in the binary number n is 1. In this case, the signal photon goes through all switches exactly once. Then, the transmission coefficient V_n assigned to the nth time bin can be written as

$$V_n = V_b V_d^{N-n} V_s^{m+1}, \tag{3}$$

where $m = \lceil \log_2 N \rceil$ and $\lceil x \rceil$ represent the ceiling function that maps its argument x to the smallest integer larger than or equal to x.

It is worth mentioning here that the combination of spatial and temporal multiplexing was also proposed in the literature [23,48,65,122,123]. SPSs based on combined multiplexing can outperform those based on any of the multiplexing schemes [48].

Another promising type of multiplexing is relative multiplexing that aims at synchronizing multiple photons at a convenient time bin, or in the spatial mode that requires the least switching [124–126]. This solution is useful in experiments where such synchronized indistinguishable photons are needed.

3.3. Spectral Multiplexing

Recently, a novel type of multiplexed sources called spectrally multiplexed SPS has been proposed and demonstrated experimentally [68,69,71,72]. In this approach, spectral modes are defined within the broadband spectrum of a photon pair source based on spontaneous parametric down-conversion. The spectral modes of the idler beam are demultiplexed into distinct modes before detection. Demultiplexing can be realized, e.g., by diffraction gratings [68,69,71] or a dense wavelength division multiplexer [72]. After detecting the idler photons in one of the spectral modes, a feedforward frequency-shift operation is applied to the heralded photons, thus switching signal photons between modes. The frequency of the heralded signal photon from the spectral mode corresponding to the frequency of the detected idler photon is shifted to the prescribed frequency ν_{out} of the output mode. Figure 3 shows the scheme of spectral multiplexing. The frequency of the signal photon can be shifted by using various techniques such as a linear phase ramp realized by an integrated phase modulator [68], four-wave mixing applying different pump frequencies [69], or a travelling wave electro-optic phase modulator [71,72]. The advantage of spectral multiplexing is that the optical switch realizing the frequency shift has a given loss, and it is not scaled up with the number of multiplexed spectral modes. However, multiplexing several spectral modes can be technically challenging. Moreover, demultiplexing of the idler beam introduces additional losses.

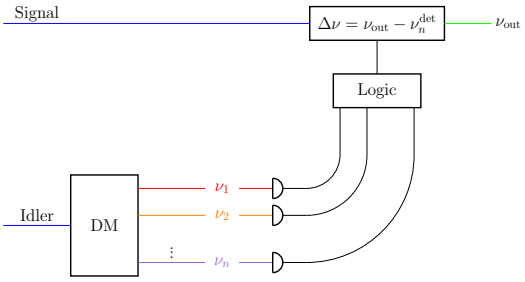

Figure 3. Schematic figure of spectral multiplexing. The demultiplexer (DM) filters the idler photons into distinct spectral modes. The frequency shift $\Delta\nu$ on the signal photons is realized depending on the detected frequency ν_n^{det}.

4. Theory of Multiplexed Single-Photon Sources

In principle, in an ideal multiplexed system free of losses, increasing the number of multiplexed units and at the same time decreasing the mean number of the generated photon pairs yields single-photon probabilities that tend to one asymptotically. However, in real multiplexed systems, all the optical constituents applied in the multiplexing system and the heralding stage have losses. In order to analyze multiplexed SPSs, theoretical descriptions are required that are capable of taking into account these losses. In Refs. [39,46,47,49], mathematical descriptions of temporally multiplexed SPSs based on storage loops were presented. Theoretical analyses of temporally multiplexed SPSs based on binary-divided delays were outlined in Refs. [40,44,51]. Theoretical models describing spatially multiplexed SPSs were developed in Refs. [41,43,45].

A full statistical theory describing any type of multiplexed SPSs was introduced in Ref. [42]. That theory can be used to determine the output probability distribution of the photon numbers of the multiplexed system for any type of input photon statistics of the photon pairs generated in the multiplexed units. It assumes threshold, that is, click detectors for heralding in the units and includes all relevant loss mechanisms. Recently, this theory has been extended to include the application of photon-number-resolving detectors capable of realizing any type of detection strategy and the possibility of using different mean numbers of the generated photon pairs λ_n in different multiplexed units [50,52]. Photon-number-resolving detectors were used in recent multiplexed SPS experiments [59,62–64,66,67,70]. The significance of the theory is that it can be used to optimize any multiplexed SPS characterized by a certain set of the loss parameters of the system, thus determining the

optimal number of multiplexed units and the optimal mean number of the photon pairs generated in the multiplexed units for which the single-photon probability is maximal. The theory can also be applied to determine the normalized second-order autocorrelation $g^{(2)}(0)$ characterizing the multiphoton contribution at the output of the multiplexed system. In the following, we summarize this extended statistical theory.

Assume that a certain type of multiplexer contains N multiplexed units and that l photon pairs are generated by the nonlinear source in the nth multiplexed unit. Furthermore, assume that only when a photon-number-resolving detector detects a predefined number of photons j ($j \leq l$) will the corresponding input ports of the multiplexer be open. Then, the probability of the arrival of i signal photons at the output of the multiplexer takes the form

$$\begin{aligned} P_i^{(S)} = &\prod_{k=1}^{N} \left(1 - \sum_{j \in S} P_k^{(D)}(j)\right) \delta_{i,0} \\ &+ \sum_{n=1}^{N} \left[\prod_{k=1}^{n-1} \left(1 - \sum_{j \in S} P_k^{(D)}(j)\right)^{(1-\delta_{1,n})} \sum_{l=i}^{\infty} \sum_{j \in S} P^{(D)}(j|l) P_n^{(\lambda_n)}(l) V_n(i|l) \right]. \end{aligned} \tag{4}$$

The formula contains various probabilities corresponding to different events.

The probability $P_n^{(\lambda_n)}(l)$ corresponds to the event that the nonlinear source in the nth multiplexed unit generates l photon pairs, with the mean number of the generated photon pairs set to λ_n in the chosen unit. There are two probability distributions that can be assumed to be related to the SPSs. In the case of multimode spontaneous parametric down-conversion or spontaneous four-wave mixing processes, that is, for weaker spectral filtering [59,64,77–81], Poissonian distribution can be assumed. In this case,

$$P_n^{(\lambda_n)}(l) = \frac{\lambda_n^l e^{-\lambda_n}}{l!}, \tag{5}$$

where λ_n represents the mean number of photon pairs originating from the nonlinear source in the multiplexed units, so it is the input of the heralding process. In the following, the term input mean photon number is used for this quantity.

The other distribution assumed in the literature is thermal distribution that is valid for the single mode, i.e., spectrally narrow-filtered spontaneous parametric down-conversion or spontaneous four-wave mixing processes. The probability of having n photon pairs in the case of thermal distribution can be expressed as

$$P_n^{(\lambda_n)}(l) = \frac{\lambda_n^l}{(1+\lambda_n)^{1+l}}. \tag{6}$$

Multiplexed SPSs in which thermal distribution is assumed can yield highly indistinguishable single photons required for the realization of various optical quantum information experiments. We note that the entangled two-mode output state of these systems determines the actual photon distribution of the photon pair generation [78].

The conditional probability $P^{(D)}(j|l)$ describes the event that j photons are registered provided that l photons fall onto the detector ($j \leq l$). Characterizing the detector by the detector efficiency V_D, this probability can be written as

$$P^{(D)}(j|l) = \binom{l}{j} V_D^j (1 - V_D)^{l-j}. \tag{7}$$

Another detection-related quantity is the probability $P_n^{(D)}(j)$ corresponding to the event that exactly j photons are detected in the nth multiplexed unit. Using the above two probabilities $P^{(D)}(j|l)$ and $P_n^{(\lambda_n)}(l)$, one can write

$$P_n^{(D)}(j) = \sum_{l=j}^{\infty} P^{(D)}(j|l) P_n^{(\lambda_n)}(l). \tag{8}$$

Refs. [42,50,52] introduce the three versions of the statistical description of multiplexed SPSs, where no other detector imperfections were taken into consideration but the finite detector efficiency described by V_D. It was also stated that omitting other imperfections poses no significant limitation against the realistic nature of the model [50]. We note that the effect of the dark counts on the performance of temporally multiplexed SPSs was analyzed in Ref. [127].

Lastly, $V_n(i|l)$ is the conditional probability quantifying the likelihood of the event that i photons leave the multiplexer provided that l signal photons arrive to the system from the nth multiplexed unit. It can be calculated as

$$V_n(i|l) = \binom{l}{i} V_n^i (1 - V_n)^{l-i}, \tag{9}$$

where V_n denotes the total transmission coefficient characterizing the losses of the nth arm of the multiplexer.

In the case of heralding events occurring in multiple multiplexed units, the preferred unit in Equation (4) is the one the sequential number n of which is the smallest. The unit controlling the operation of the switches of the multiplexer should implement this priority logic. Hence, the total transmission coefficients V_n describing the losses experienced by the photons in the arms of the multiplexer are to be sorted into a descending order for a given set of the loss parameters. Such a renumbering ensures that the multiplexer arm characterized by the highest V_n that corresponds to the smallest loss is favored by the priority logic in the case of multiple heralding events occurring in the system [50,53]. In this way, the probability that the input signal photon vanishes in the multiplexer is reduced; hence, the output single-photon probability is higher.

The set S contains the number of photons detected in a multiplexed unit that triggers the opening of the corresponding input port of the multiplexer to let the generated signal photons into it. Assuming that such a set allows for using an optional detection strategy that cannot be realized without a photon-number-resolving detector, the elements of the set S are positive integers less than or equal to a value J_b characterizing the resolving capability of the photon-number-resolving detector: this number is the highest number of photons that can still be distinguished by the detector. Such a detector can also be used as a threshold detector by assuming the set S to contain all positive integers.

There are two terms in Equation (4). The first one quantifies the likelihood of detecting an unexpected number of photons, that is, the number of photons registered in the multiplexed unit is outside the set S. Considering that for an unexpected number of photons detected in a multiplexed unit the corresponding input port of the multiplexer does not open, this first term contributes to the probability $P_0^{(S)}$ of obtaining no outgoing photons from the multiplexer. Consequently, all events corresponding to the detection of an expected number of photons in a multiplexed unit are described by the second term. Here, it is assumed that l photons enter the multiplexer from the nth unit subsequent to the heralding, but the output is reached by only i of these photons owing to the losses present in the multiplexer. In this term, the first factor expresses the fact that no expected number of photons is detected in the first $n-1$ multiplexed units.

The theory can also be used to characterize the multiphoton contribution at the output of the multiplexed system. This is generally quantified by the normalized second-order autocorrelation function [23]

$$g^{(2)}(0) = \frac{\sum_{i=2}^{\infty} P_i^{(S)} i(i-1)}{\left(\sum_{i=1}^{\infty} P_i^{(S)} i\right)^2} \tag{10}$$

that measures the multiphoton components of the output state relative to the single-photon component. In this formula, the probabilities $P_i^{(S)}$ $(i = 1, 2, \dots)$ of obtaining i photons at the output can be calculated by using Equation (4).

Next, we summarize how the theoretical description can be used to optimize a given multiplexed system. As it was stated before, Equation (4) can be used to determine the probability of getting a single signal photon at the output of the multiplexer. After fixing the values of the various losses characterizing the multiplexed SPS such as the transmission coefficients V_r and V_t of the individual routers building up the spatial multiplexer or, in the case of temporal multiplexing, the corresponding quantity V_S characterizing the switch, the detector efficiency V_D, and the general transmission coefficient V_b, Equation (4) still contains two free parameters, or variables, namely, the number of multiplexed units N and the input mean photon number λ. Note that the formula allows for the use of different input mean photon numbers λ_n in the various multiplexed units, which means that the number of variables in Equation (4) is $N + 1$, namely, the input mean photon numbers λ_n, $n = 1, \dots, N$ and the number of multiplexed units N. Then, the optimization of a given multiplexed system means determining the optimal values of these variables, that is, the optimal number of multiplexed units N_{opt} and the optimal input mean photon number or numbers λ_{opt} or $\lambda_{n,\mathrm{opt}}$, respectively, for which the value of the single-photon probability $P_{1,\mathrm{max}}$ is maximal. This can be accomplished in two steps. First, the number of multiplexed units N is fixed, and the input mean photon number λ or, generally, photon numbers λ_n have to be determined for which the single-photon probability P_1 is maximal. As it is shown in the next section, the single-photon probability function depending on the input mean photon number λ always has a well-defined maximum that can be found by applying standard optimization algorithms such as the gradient method. In the case of different input mean photon numbers λ_n, other optimization methods such as the genetic algorithm can be used. Such optimization algorithms are available in several mathematical software packages. Next, this method is applied for all reasonable values of the number of multiplexed units N, thus obtaining $P_1 - N$ pairs forming a discrete function. In the case of SPSs based on certain types of multiplexers, this discrete function has a single maximum that can be selected easily. Examples of such multiplexers are the symmetric multiplexer and the temporal multiplexer based on binary-divided delays [42,51]. For SPSs based on other types of multiplexers, the discrete function has a well-defined global maximum, but it can contain local maxima as well. In this case, it is still possible to select the global maximum. Input- or output-extended incomplete binary tree multiplexers are representative examples of such multiplexers [53,54]. Finally, the discrete function might have no global maximum at all; instead, it tends to a finite value less than one as the number of multiplexed units is increased. This behavior is characteristic of SPSs based on asymmetric and stepwise-optimized binary tree multiplexers [52,55] and for temporal multiplexers based on storage loop delays [37,39,47,49]. Obviously, when choosing well-defined optimal system parameters in this case is not possible, one of the following two approaches can be applied instead. In the first approach, the single-photon probability P_1 is maximized for a sufficiently high number of multiplexed units N_{high}, leading to $P_{1,N_{\mathrm{high}}}$, and it is considered to be close to the saturated value. Then, the highest single-photon probabilities $P_{1,N}$ are determined for lower values of the number

of multiplexed units, and they are compared to the highest single-photon probability $P_{1,N_{\text{high}}}$ found for the high number of multiplexed units. In this case, the lowest value of the number of multiplexed units N for which the difference $P_{1,N_{\text{high}}} - P_{1,N}$ is smaller than a predefined value is said to be the optimal number of multiplexed units N_{opt}, the input mean photon numbers that yield $P_{1,N}$ are called the optimal input mean photon numbers λ_n, and $P_{1,N}$ is called the maximal single-photon probability $P_{1,\text{max}}$. In the second approach, the highest single-photon probabilities obtained for neighboring values N and $N-1$ of the number of multiplexed units are compared. In this case, the lowest value N for which the difference $P_{1,N} - P_{1,N-1}$ is smaller than a predefined value is called the optimal number of multiplexed units N_{opt}, the input mean photon numbers that yield $P_{1,N}$ are called the optimal input mean photon numbers λ_n, and $P_{1,N}$ is called the maximal single-photon probability $P_{1,\text{max}}$.

5. Theoretical Results and Experiments

5.1. Theoretical Results

The performance outcomes of various SPSs have been discussed in Refs. [39–41,43–47,49,51] applying different theoretical models. Using the general theoretical description outlined in the previous section, the properties and characteristics of SPSs based on different multiplexing methods have been analyzed in Refs. [42,48,50,52–57]. According to these analyses, it can be stated for all multiplexed SPSs that the performance of the system improves for lower system losses, that is, for higher values of the various transmission coefficients and efficiencies. Also, the single-photon probability of multiplexed sources can be increased by using photon-number-resolving detectors [50]. We assume that higher values of the detector efficiency of such detectors lead to higher single-photon probabilities and, simultaneously, lower values of the multiphoton noise. Assuming thermal statistics for the distribution of the generated photon pairs required for the indistinguishability of the generated photons, the resulting output single-photon probabilities are lower than those for Poissonian statistics [53]. Another common characteristic of multiplexed SPSs is that the single-photon probability plotted against the input mean photon number exhibits a single maximum for any value of the number of multiplexed units N. This is shown in Figure 4 for SPSs based on five different types of multiplexers and for $N = 10$ multiplexed units. The maximum shifts toward smaller values of the input mean photon number λ with increasing values of the number of multiplexed units N [42,50,57]. The physical reason behind these observations is that when the input mean photon number λ is low, the likelihood of not obtaining any photons at the output of the system is high, while high values of λ lead to increased multiphoton contribution. The shifting of the maximum can be explained by the fact that the assumption of higher values of the number of multiplexed units N allows for the use of lower values of the input mean photon number λ to retain the probability of successful heralding high in the whole system. Knowing the maxima of the $P_1(\lambda)$ functions for all reasonable values of N, one can determine the optimal value N_{opt} together with the optimal values of λ_{opt} for which the single-photon probability is the highest, as described in the previous section. This value is called the maximal single-photon probability $P_{1,\text{max}}$ that can be achieved with the considered SPS.

Table 1 shows examples for the maximal single-photon probability $P_{1,\text{max}}$, the corresponding values of the normalized second-order autocorrelation function $g^{(2)}$, and the optimal values of the number of multiplexed units N_{opt}, as well as the input mean photon number λ_{opt} for SPSs based on five different types of multiplexers: an asymmetric multiplexer (ASYM) [52], stepwise-optimized binary tree multiplexers (SOBTMs) [55], minimum-based, maximum-logic output-extended incomplete binary tree multiplexers (OMAXVs) [54], and temporal multiplexers based on binary-divided delays (binary-divided) and on storage loops (loop) for two sets of loss parameters. With the aim of comparing the performance of the various spatially and temporally multiplexed SPSs, we have calculated all the values shown in the table for the same sets of parameters. The first parameter set characterizes

state-of-the-art optical devices and elements [70,119,128]. The second set comprises parameters that can expectedly be realized in multiplexed SPS experiments. Exact values of the parameters are listed in the table caption. Note that corresponding calculation results for temporally multiplexed SPSs can be found for different parameter sets in Refs. [42,50]. To obtain the data presented in the table for SPSs based on temporal multiplexers, we have used Equations (2) and (3).

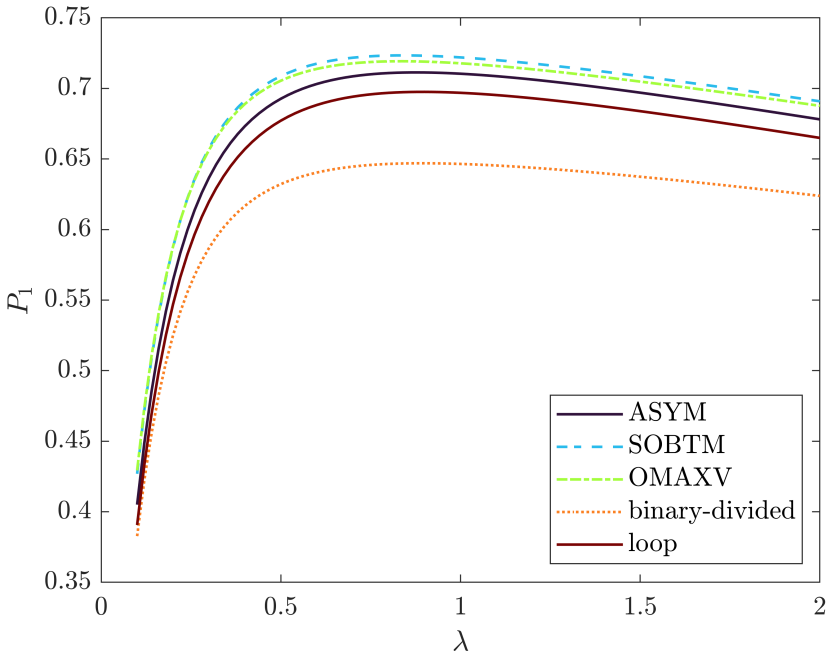

Figure 4. Single-photon probability P_1 as a function of the input mean photon number λ for SPSs based on five different types of multiplexers: asymmetric multiplexer (ASYM), minimum-based, maximum-logic output-extended incomplete binary tree multiplexers (OMAXVs), stepwise-optimized binary tree multiplexers (SOBTMs), temporal multiplexers based on binary-divided delays (binary-divided) and on storage loops (loop), for the number of multiplexed units $N = 10$, the transmission coefficients $V_r = 0.95$ and $V_t = 0.95$, the general transmission coefficient $V_b = 0.95$, the detector efficiency $V_D = 0.9$, and, in the case of temporal multiplexers, the transmission coefficient of one-time-bin delay $V_d = 0.99$, as well as when the loss characterizing a switch is $V_s = 0.95$.

Table 1. Comparison of the performances of SPSs based on various temporal and spatial multiplexer structures for two sets of loss parameters. State-of-the-art parameters: transmission coefficients $V_r = 0.99$, $V_t = 0.985$, detector efficiency $V_D = 0.95$, general transmission coefficient $V_b = 0.98$. Realistic parameters: transmission coefficients $V_r = 0.95$, $V_t = 0.95$, detector efficiency $V_D = 0.9$, general transmission coefficient $V_b = 0.95$. In both cases for temporal multiplexers, the transmission coefficient of one-time-bin delay is $V_d = 0.99$, and the loss values characterizing a switch in the two cases are $V_s = 0.99$ and $V_s = 0.95$, respectively.

	State-of-the-Art				**Realistic**			
Type	$P_{1,max}$	$g^{(2)}$	N_{opt}	λ_{opt}	$P_{1,max}$	$g^{(2)}$	N_{opt}	λ_{opt}
Spatial ASYM	0.905	0.061	31	0.453	0.739	0.166	23	0.757
Spatial SOBTM	0.916	0.041	42	0.259	0.763	0.128	29	0.500
Spatial OMAXV	0.913	0.039	39	0.249	0.749	0.128	21	0.502
Temporal binary-divided	0.867	0.063	32	0.472	0.679	0.156	16	0.685
Temporal loop	0.881	0.076	24	0.637	0.722	0.174	20	0.809

The table shows that the differences between maximal single-photon probabilities $P_{1,max}$ that can be obtained with SPSs based on these multiplexers are moderate for the

parameter sets used. However, the required optimal numbers of multiplexed units N_{opt} and the corresponding values of the normalized second-order autocorrelation function $g^{(2)}$, as well as the optimal input mean photon numbers λ_{opt}, are considerably different. The highest single-photon probability that can be achieved both for state-of-the-art parameters and for realistic parameter sets can be obtained with SPSs based on SOBTMs. Generally, the relation between the performances of SPSs based on different multiplexing methods depends on the chosen sets of the loss parameters. A detailed comparison of SPSs based on OMAXVs and asymmetric multiplexers in this respect can be found in Ref. [54]. That analysis shows that, though SPSs based on OMAXVs surpass those based on asymmetric multiplexers in the present examples, in the case of multiplexers built of highly asymmetric photon routers, SPSs based on asymmetric multiplexers usually show better performance than those based on OMAXVs.

The optimization of SPSs usually means maximizing the single-photon probability. Note, however, that the highest single-photon probabilities obtained by the optimization are not necessarily accompanied by low values of the second-order autocorrelation function. In Ref. [57], a method was proposed to reduce the multiphoton contribution of a multiplexed SPS with a moderate reduction in the single-photon probability compared to the maximal one obtained from the optimization above. In that paper, it was shown that the relation between the normalized second-order autocorrelation function $g^{(2)}$ and the input mean photon number λ is practically linear. Hence, the reduction of λ results in a decrease in $g^{(2)}$, but this also leads to a reduction in the single-photon probability P_1. The solution to this problem is the reoptimization of the system, that is, determining the optimal number of multiplexed units and optimal input mean photon numbers for the prescribed lower value of the normalized second-order autocorrelation function for which the reduction of the single-photon probability is minimal.

The theoretical analyses also showed that the optimal system sizes, that is, the optimal numbers of multiplexed units, are higher, and the optimal input mean photon numbers are lower for lower losses of the multiplexer [52,53]. In contrast, for higher detector efficiencies V_D, the values of the optimal input mean photon number λ_{opt} are higher, while the corresponding values of the optimal number of multiplexed units N_{opt} are lower. Obviously, in the case of higher losses of the multiplexer, keeping the system sizes at high values increases the probability that the photon vanishes in the multiplexer. Also, applying a better photon-number-resolving detector for heralding can better suppress the multiphoton contribution in the signal entering the multiplexer.

The performance of multiplexed SPSs can be further improved by using different input mean photon numbers in the different multiplexed units [41,52,56]. This method takes into account that different arms of the multiplexer generally introduce different losses. In Ref. [41], a definite functional dependence for the different input mean photon numbers was proposed. The idea of using different input mean photon numbers was inserted into the general theory of multiplexed sources in Ref. [52]. The theory presented in the previous section includes this possibility. The optimal values of the different input mean photon numbers can be determined by using standard multivariate optimization methods such as the genetic algorithm. The theory has been applied for SPSs based on asymmetric multiplexers [52] and for those based on OMAXVs [56]. It was shown that the method applying a full optimization for all the individual input mean photon numbers surpasses the one assuming a functional dependence for the different input mean photon numbers.

The application of photon-number-resolving detectors in the multiplexed units has opened the possibility to optimize multiplexed SPSs in which a heralding strategy can be chosen based on the actual number of detected photons [50,52,53]. The theory shown in Section 4 also includes this possibility. The analyses showed that for multiplexers with higher losses, it can be advantageous to choose a strategy in which two or more photons also induce a heralding event [50,52,53].

The theoretical models described above and proposed in the literature were also used to analyze multiplexed SPSs with suboptimal system sizes, that is, for the number of mul-

tiplexed units less than what would be optimal for a given set of loss parameters [52–55]. The relevance of analyzing SPSs with suboptimal system sizes is that using relatively low, suboptimal number of optical elements is the typical situation in experiments realized so far [58,59,61,63,64]. Next, we present results that show the typical behavior of multiplexed SPSs for suboptimal system sizes. Figure 5 shows the characteristics of SPSs based on the multiplexers presented in Table 1 for suboptimal values of the number of multiplexed units. The three subfigures show the maximal single-photon probability $P_{1,N}$ (a), the corresponding values of the normalized second-order autocorrelation function $g_N^{(2)}$ (b), and the optimal input mean photon number $\lambda_{\mathrm{opt},N}$ (c) against the number of multiplexed units N. The loss parameters of the multiplexed systems for which the data are shown in the figure are the realistic ones used in Table 1. Note that $P_{1,N}$ is maximal, and $\lambda_{\mathrm{opt},N}$ is optimal only for the chosen value of N. Figure 5a shows that increasing the number of multiplexed units N (but still keeping it below the optimal value), where the maximal single-photon probability $P_{1,N}$ increases in general. We point out, however, that in the case of spatially multiplexed SPSs based on OMAXVs and for temporally multiplexed SPSs based on binary-divided delays, there can be breaking points [40,53]. It is also worth noting that single-photon probabilities higher than 0.7 can be obtained by applying four of these multiplexers in an SPS with only $N = 11$ multiplexed units, while for temporally multiplexed SPSs based on binary-divided delays, this value is higher than 0.65. This observation shows that it is possible to achieve high single-photon probabilities close to the maximal value with a considerably lower number of multiplexed units than the optimal value. According to the figure, the highest single-photon probabilities $P_{1,N}$ can be obtained for SPSs based on stepwise-optimized binary tree multiplexers for all values of the number of multiplexed units. Figure 5b shows that an increasing number of multiplexed units N yields decreasing values of the normalized second-order autocorrelation function $g_N^{(2)}$ for all multiplexer types. The lowest, that is, best values of $g_N^{(2)}$ can be obtained for SPSs based on OMAXV multiplexers. Finally, Figure 5c shows that, similarly to the $g^{(2)}$ function, the optimal input mean photon number $\lambda_{\mathrm{opt},N}$ decreases with increasing numbers of multiplexed units N. Figure 5b,c, show that there is a correlation between the normalized second-order autocorrelation function and the input mean photon number, as we have discussed above. We note that for suboptimal system sizes, the application of different input mean photon numbers in the multiplexed units can relevantly improve the performance of the underlying SPS [52,56].

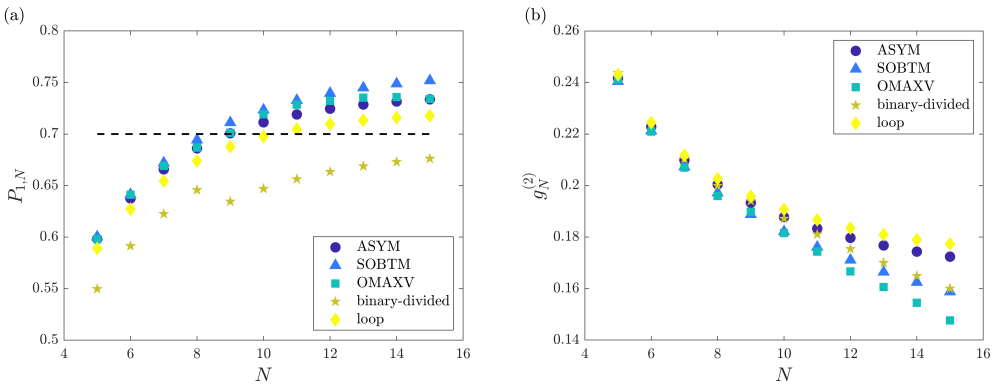

Figure 5. *Cont.*

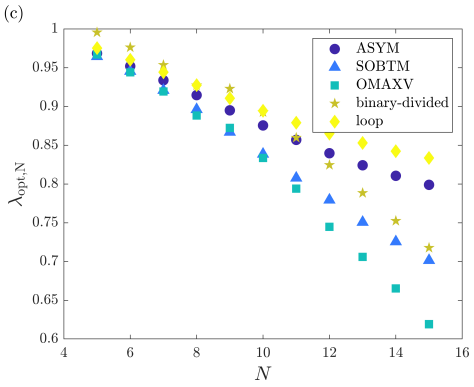

Figure 5. (**a**) Achievable single-photon probability $P_{1,N}$, (**b**) normalized second-order autocorrelation function $g_N^{(2)}$, and (**c**) optimal input mean photon number $\lambda_{\mathrm{opt},N}$ against the number of multiplexed units N for SPSs based on five different types of multiplexers: asymmetric multiplexer (ASYM), stepwise-optimized binary tree multiplexers (SOBTMs), minimum-based, maximum-logic output-extended incomplete binary tree multiplexers (OMAXVs), temporal multiplexers based on binary-divided delays (binary-divided) and on storage loops (loop) for the transmission coefficients $V_r = 0.95$ and $V_t = 0.95$, the detector efficiency $V_D = 0.9$, the general transmission coefficient $V_b = 0.95$, and in the case of temporal multiplexers, the transmission coefficient of one-time-bin delay $V_d = 0.99$ and the loss characterizing a switch at $V_s = 0.95$.

5.2. Multiplexed Single-Photon Source Experiments

Though the idea of multiplexed SPSs is quite straightforward, the first experimental realization of such a source based on spatial multiplexing of four multiplexed units was reported only in 2011 [58]. In that experiment, a pair of beta barium borate crystals were used as parametric down-conversion sources, and the routing of the heralded photons to the output was realized by a fast, Pockels cell-based electro-optic polarization rotating switch. Multiplexing four heralded photon sources based on parametric down-conversion in waveguides was reported in 2016 [61]. In this experiment, integrated electro-optic switches were used. The advantage of using photon-number-resolving detectors in a multiplexed SPS experiment was presented in Ref. [64]. That experiment realized spatial multiplexing of two heralded sources based on spontaneous parametric down-conversion in bulk crystals. Experimental realizations of spatial multiplexing have also been reported for up to two multiplexed units by using spontaneous four-wave mixing in photonic crystal fibers and integrated opto-ceramic switches [59,60,63]. In all these experiments, symmetric multiplexers were used. The cited experiments successfully demonstrated the usefulness of multiplexing, though they could not exceed the overall performance of a single heralded source due to the high losses of the realized multiplexed systems.

Concerning SPSs based on temporal multiplexing, six experimental realizations have been reported in the literature. In Refs. [66,67], fiber-based systems with spontaneous four-wave mixing and integrated switches were used to realize temporally multiplexed SPSs based on storage loops with four time bins. Temporally multiplexed SPSs based on free-space storage cavities were realized by applying spontaneous parametric down-conversion for pair generation and using large-scale temporal multiplexing up to 30 [62] and 40 [70] time bins. In these experiments, low-loss Pockels cell-based optical switches were used. The scheme of the applied storage cavity is shown in Figure 6.

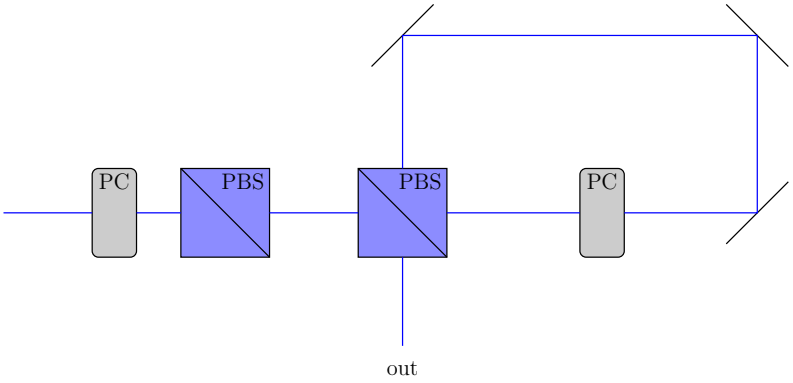

Figure 6. Schematic figure of a storage cavity with Pockels cell-based optical switches. PBSs denote polarizing beam splitters; PCs are Pockels cells.

In the scheme, the leftmost Pockels cell used to set up the polarization of the signal photon so that the neighboring polarization beam splitter either directs the photon into the storage cavity or discards it. The polarizations of the photons directed into the storage cavity are adjusted by the Pockels cell on the right so that the polarization beam splitter, which is part of the cavity, can direct the photon either to the output or back to the cavity. In the experiment of Ref. [70], an output single-photon probability $P_1 = 0.67$ was reported that is considerably higher than that can be achieved with heralded SPSs. This single-photon probability is even higher than the best values reported for SPSs based on quantum dots [57,129–133]. We note, however, that the normalized second-order autocorrelation value $g^{(2)} = 0.27$ obtained in this experiment is higher, that is, worse, compared to the value $g^{(2)} \approx 0.02$ achieved in the cited quantum-dot based SPS experiments. Accordingly, the fidelity of the output photon state is lower for this multiplexed source due to the higher multi-photon contribution. Note that there is a tradeoff between the second-order autocorrelation function $g^{(2)}$ and the single-photon probability P_1. The value of $g^{(2)}$ can be reduced by decreasing the input mean photon number λ, which generally leads to a decrease in the single-photon probability P_1. This decrease can be reduced by the reoptimization method described in Section 5.1 and originally introduced in Ref. [57].

In a recent experiment, a telecom wavelength temporally multiplexed integrated SPS based on a silicon waveguide and a low-loss fiber switch and loop architecture has been presented [134]. In this experiment, a value $g^{(2)}(0) = 0.01$ of the normalized second-order autocorrelation function was achieved, which is comparable to the values obtained with quantum dot sources. The single-photon probability of this source was rather low ($P_1 \approx 0.015$), though this system achieved a factor 4.5 ± 0.5 enhancement of the single-photon probability of the heralded source used. In Ref. [135], a telecom wavelength continuous wave temporally multiplexed SPS based principally on fiber-integrated components and applying two time bins was demonstrated. The latter two experiments are important steps toward the development of integrated telecom-wavelength SPSs that can be applied in practical quantum communication.

Combined multiplexing was also successfully realized in an experiment reported in Ref. [65]. In that experiment, two heralded SPSs based on parametric down-conversion were multiplexed spatially and then temporally using binary-divided delay lines realizing four time bins.

Regarding spectrally multiplexed SPSs, four experimental realizations have been published thus far [68,69,71,72]. In these experiments, only three spectral modes have been multiplexed, probably because increasing the number of multiplexed spectral modes can be technically challenging.

Finally, we note that all the available experimental data concerning the multiplexed experiments reviewed here have been presented in a table of Ref. [9] except for data of the experiments presented in Refs. [134,135]. In addition to the single-photon probability (brightness) of the source and the second-order correlation function, the single-photon rate

is an important data measurement characterizing SPSs. The best value of the single-photon rate (130 kHz) was achieved with the temporally multiplexed SPS of Ref. [70] that also produced the highest single-photon probability ($P_1 = 0.67$), as was pointed out above.

The experiments reviewed in this section used various types of sources, switches, and detectors. All these elements are available both in bulk optic and integrated forms. A detailed evaluation and comparison of the different realizations of these elements can be found in Ref. [9]. As we have described earlier, the performance of a multiplexed SPS is basically determined by the losses of the components forming the multiplexed units and the multiplexer. The losses of integrated switches are significantly higher than those of bulk switches, but they can be faster than the bulk ones. Additional losses appear in integrated sources when disparate elements are coupled and also at coupling of bulk optic elements to integrated ones. Nevertheless, integrated optical devices can be easily adapted to practical applications due to their compactness and robustness. Hence, the development of multiplexed SPSs realized with integrated optical elements is an important research topic.

5.3. Application of Single-Photon Sources

Single photons can be used as qubits encoding the quantum information in any of its degrees of freedom, for example, path, polarization, or time bin. They are largely free of noise or decoherence and can be easily manipulated. In the fields of quantum information processing and photonic quantum technology, there are several experiments and numerous applications where SPSs are key elements [1–6].

One group of them are quantum key distribution (QKD) protocols that ensure the secure generation of keys between two points of a communication network [136–141]. A widely adapted protocol is BB84, which is based on the transmission and measurement of individual photons [142]. QKD systems have already been realized and used in practice [143–147]. Note that these systems generally apply laser systems, which generate weak coherent states instead of single photons. Nevertheless, the application of real SPSs would increase the security level and their efficiency. The performance of multiplexed SPSs in a practical QKD implementation has been analyzed in Ref. [148] by evaluating the achievable key rates.

Another type of quantum communication is quantum teleportation that aims at transferring a quantum state between distant nodes of a network [149,150]. Quantum teleportation of photonic qubits has been successfully performed in several experiments [151–156].

SPSs are fundamental building blocks in linear optical quantum computing [1,4,5,157] Multiplexed SPSs are good candidates to meet all the criteria needed for the practical realization of this type of computing. These requirements, that is, high fidelity ($g^{(2)} < 0.07$) and single-photon probability ($P_1 > 0.9$), were determined in Ref. [158]. Another type of quantum computing is one-way quantum computing, which is based on the generation of a highly entangled cluster state [1,3–5,159–162]. In this approach, the computation is performed by a processing circuit consisting only of single-qubit measurements and feedforward operations.

Though cluster states are generally prepared by using entangled photon pair sources [163–168], SPSs can be also used for their efficient preparation [169–173].

Boson sampling is a non-universal photonic quantum computing protocol where quantum computation supremacy over classical computers can be demonstrated [174]. Boson sampling has been realized successfully in several experiments [130,175–178]. Multiple indistinguishable single-photon inputs of boson sampling scheme can be ensured by demultiplexing of the stream of photons of the SPS [179].

Quantum memories in which the state of photonic qubits generated by SPSs can be stored are important elements of several optical quantum protocols [180–188]. One type of optical quantum memories is based on storage loops or cavities used in temporally multiplexed SPSs [180,184,185,187–189].

In addition to these applications in quantum information processing, efficient SPSs producing single-photon states are also assumed in several quantum optical schemes for

generating quantum states of light [190–198] and in experiments investigating the quantum nature of light [199,200].

Finally, we note that in the experiments and in the applications realized in practice in the reviewed areas of applications, quantum dot-based or heralded SPSs have been used. The practical application of multiplexed SPSs in these areas is hindered by the fact that such sources have been realized experimentally only in laboratories; presently, no compact version of them is available.

6. Discussion

In this review, we have summarized the progress in multiplexed single-photon sources. Special attention has been paid to the detailed presentation of the recent theoretical results that can help the experimental realization of high-performance single-photon sources.

The theoretical results show and successful experiments demonstrate that multiplexed single-photon sources can produce highly indistinguishable single photons in near-perfect spatio-temporal modes with known polarization and with a high single-photon probability in a pseudo-deterministic way. Multiplexed sources can produce single photon signals with higher single-photon probabilities accompanied by lower multi-photon contribution compared to a heralded source alone. The performance of a multiplexed single-photon source is determined by the losses of the system such as the losses of the switching elements and the delay lines and the efficiencies of the detectors for heralding. There has been remarkable progress in the field of producing low-loss optical elements and devices that will probably proceed. For example, photon-number-resolving detectors with high detector efficiencies and low dark counts are now available for experiments. Obviously, a system characterized by lower losses can produce higher single-photon probabilities. According to the theoretical analyses, by using optical elements characterized by the same parameters in a multiplexed single-photon source, the application of different multiplexing types and schemes in a single-photon source can result in different performances. The actual set of loss parameters determines which of the multiplexing schemes will provide the highest performance single-photon source.

The most important result of the theoretical analysis of multiplexed single-photon sources is that they can be optimized, that is, it is possible to determine optimal values for the system size and the number of photon pairs generated in the multiplexed units for which the output single-photon probability is maximal. The optimal system size is generally lower when detectors with higher efficiencies are used in the multiplexed units. The single-photon probability can be further increased by the unit-wise optimization of the number of generated photon pairs. The multiphoton contribution at the output of a multiplexed single-photon source can be decreased by decreasing the input mean photon number in the multiplexed units. This leads to a decrease in the single-photon probability that can be minimized by determining a novel optimal system size by reoptimizing the system. The theoretical analyses also showed that high single-photon probabilities can be achieved even for suboptimal system sizes with optimized input mean photon numbers.

Successful multiplexed single-photon source experiments have demonstrated the usefulness of multiplexing, but most of them have not produced single-photon probabilities high enough for most of the applications, except for the two experimentally realized temporally multiplexed single-photon sources reported in Refs. [62,70]. Several successful multiplexed source experiments have already applied integrated optical elements. Realizing fully integrated multiplexed sources is a promising future research direction as most of the applications require robust and compact single-photon sources. Advance in the development of efficient low-loss integrated optical elements is needed for proceeding in this area. Application of the summarized theoretical results in future experiments can further improve the performance of multiplexed single-photon sources.

All the reviewed theoretical and experimental results anticipate that, in the near future, multiplexed single-photon sources can meet all the criteria posed on single-photon sources by the various applications.

Author Contributions: Conceptualization, P.A.; writing—original draft preparation, M.M.; writing—review and editing, P.A. and M.M. All authors have read and agreed to the published version of the manuscript.

Funding: This research was supported by the National Research, Development and Innovation Office, Hungary ("Quantum Information National Laboratory of Hungary" Grant No. 2022-2.1.1-NL-2022-00004, "Frontline" Research Excellence Programme Grant No. KKP133827, and Grant Nos. TKP2021-NVA-04 and TKP2021-EGA-17).

Institutional Review Board Statement: Not applicable.

Informed Consent Statement: Not applicable.

Data Availability Statement: The data underlying the results presented in this paper are not publicly available at this time, but theymay be obtained from the authors upon reasonable request.

Conflicts of Interest: The authors declare no conflicts of interest.

References

1. O'Brien, J.L. Optical Quantum Computing. *Science* **2007**, *318*, 1567–1570. [CrossRef] [PubMed]
2. Chunnilall, C.J.; Degiovanni, I.P.; Kück, S.; Müller, I.; Sinclair, A.G. Metrology of single-photon sources and detectors: A review. *Opt. Eng.* **2014**, *53*, 081910. [CrossRef]
3. Flamini, F.; Spagnolo, N.; Sciarrino, F. Photonic quantum information processing: A review. *Rep. Prog. Phys.* **2019**, *82*, 016001. [CrossRef] [PubMed]
4. Slussarenko, S.; Pryde, G.J. Photonic quantum information processing: A concise review. *Appl. Phys. Rev.* **2019**, *6*, 041303. [CrossRef]
5. Couteau, C.; Barz, S.; Durt, T.; Gerrits, T.; Huwer, J.; Prevedel, R.; Rarity, J.; Shields, A.; Weihs, G. Applications of single photons to quantum communication and computing. *Nat. Rev. Phys.* **2023**, *5*, 326–338. [CrossRef]
6. Couteau, C.; Barz, S.; Durt, T.; Gerrits, T.; Huwer, J.; Prevedel, R.; Rarity, J.; Shields, A.; Weihs, G. Applications of single photons in quantum metrology, biology and the foundations of quantum physics. *Nat. Rev. Phys.* **2023**, *5*, 354–363. [CrossRef]
7. Eisaman, M.D.; Fan, J.; Migdall, A.; Polyakov, S.V. Invited Review Article: Single-photon sources and detectors. *Rev. Sci. Instrum.* **2011**, *82*, 71101. [CrossRef]
8. Cao, X.; Zopf, M.; Ding, F. Telecom wavelength single photon sources. *J. Semicond.* **2019**, *40*, 071901. [CrossRef]
9. Meyer-Scott, E.; Silberhorn, C.; Migdall, A. Single-photon sources: Approaching the ideal through multiplexing. *Rev. Sci. Instrum.* **2020**, *91*, 41101. [CrossRef] [PubMed]
10. Wang, Y.; Jöns, K.D.; Sun, Z. Integrated photon-pair sources with nonlinear optics. *Appl. Phys. Rev.* **2021**, *8*, 011314. [CrossRef]
11. Elefante, A.; Dello Russo, S.; Sgobba, F.; Santamaria Amato, L.; Pallotti, D.K.; Dequal, D.; Siciliani de Cumis, M. Recent Progress in Short and Mid-Infrared Single-Photon Generation: A Review. *Optics* **2023**, *4*, 13–38. [CrossRef]
12. Alibart, O.; Ostrowsky, D.B.; Baldi, P.; Tanzilli, S. High-performance guided-wave asynchronous heralded single-photon source. *Opt. Lett.* **2005**, *30*, 1539. [CrossRef] [PubMed]
13. Pittman, T.; Jacobs, B.; Franson, J. Heralding single photons from pulsed parametric down-conversion. *Opt. Commun.* **2005**, *246*, 545–550. [CrossRef]
14. Horikiri, T.; Takeno, Y.; Yabushita, A.; Kobayashi, T. Photon-number-resolved heralded-photon source for improved quantum key distribution. *Phys. Rev. A* **2007**, *76*, 012306. [CrossRef]
15. Goldschmidt, E.A.; Eisaman, M.D.; Fan, J.; Polyakov, S.V.; Migdall, A. Spectrally bright and broad fiber-based heralded single-photon source. *Phys. Rev. A* **2008**, *78*, 013844. [CrossRef]
16. Mosley, P.J.; Lundeen, J.S.; Smith, B.J.; Walmsley, I.A. Conditional preparation of single photons using parametric downconversion: A recipe for purity. *New J. Phys.* **2008**, *10*, 093011. [CrossRef]
17. Mosley, P.J.; Lundeen, J.S.; Smith, B.J.; Wasylczyk, P.; U'Ren, A.B.; Silberhorn, C.; Walmsley, I.A. Heralded Generation of Ultrafast Single Photons in Pure Quantum States. *Phys. Rev. Lett.* **2008**, *100*, 133601. [CrossRef]
18. Huang, Y.P.; Altepeter, J.B.; Kumar, P. Heralding single photons without spectral factorability. *Phys. Rev. A* **2010**, *82*, 043826. [CrossRef]
19. Levine, Z.H.; Fan, J.; Chen, J.; Ling, A.; Migdall, A. Heralded, pure-state single-photon source based on a Potassium Titanyl Phosphate waveguide. *Opt. Express* **2010**, *18*, 3708. [CrossRef]
20. Brida, G.; Degiovanni, I.P.; Genovese, M.; Migdall, A.; Piacentini, F.; Polyakov, S.V.; Ruo Berchera, I. Experimental realization of a low-noise heralded single-photon source. *Opt. Express* **2011**, *19*, 1484. [CrossRef]
21. Förtsch, M.; Fürst, J.U.; Wittmann, C.; Strekalov, D.; Aiello, A.; Chekhova, M.V.; Silberhorn, C.; Leuchs, G.; Marquardt, C. A versatile source of single photons for quantum information processing. *Nat. Commun.* **2013**, *4*, 1818. [CrossRef] [PubMed]
22. Ramelow, S.; Mech, A.; Giustina, M.; Gröblacher, S.; Wieczorek, W.; Beyer, J.; Lita, A.; Calkins, B.; Gerrits, T.; Nam, S.W.; et al. Highly efficient heralding of entangled single photons. *Opt. Express* **2013**, *21*, 6707. [CrossRef] [PubMed]
23. Latypov, I.Z.; Shkalikov, A.V.; Kalachev, A.A. Optimization of a heralded single-photon source with spatial and temporal multiplexing. *J. Phys. Conf. Ser.* **2015**, *613*, 012009. [CrossRef]

24. Kaneda, F.; Garay-Palmett, K.; U'Ren, A.B.; Kwiat, P.G. Heralded single-photon source utilizing highly nondegenerate, spectrally factorable spontaneous parametric downconversion. *Opt. Express* **2016**, *24*, 10733–10747. [CrossRef] [PubMed]
25. Ma, C.; Wang, X.; Anant, V.; Beyer, A.D.; Shaw, M.D.; Mookherjea, S. Silicon photonic entangled photon-pair and heralded single photon generation with CAR > 12,000 and $g^{(2)}(0) < 0.006$. *Opt. Express* **2017**, *25*, 32995. [CrossRef]
26. Ansari, V.; Roccia, E.; Santandrea, M.; Doostdar, M.; Eigner, C.; Padberg, L.; Gianani, I.; Sbroscia, M.; Donohue, J.M.; Mancino, L.; et al. Heralded generation of high-purity ultrashort single photons in programmable temporal shapes. *Opt. Express* **2018**, *26*, 2764. [CrossRef] [PubMed]
27. Massaro, M.; Meyer-Scott, E.; Montaut, N.; Herrmann, H.; Silberhorn, C. Improving SPDC single-photon sources via extended heralding and feed-forward control. *New J. Phys.* **2019**, *21*, 053038. [CrossRef]
28. Li, J.; Su, J.; Cui, L.; Xie, T.; Ou, Z.Y.; Li, X. Generation of pure-state single photons with high heralding efficiency by using a three-stage nonlinear interferometer. *Appl. Phys. Lett.* **2020**, *116*, 204002. [CrossRef]
29. Lugani, J.; Francis-Jones, R.J.A.; Boutari, J.; Walmsley, I.A. Spectrally pure single photons at telecommunications wavelengths using commercial birefringent optical fiber. *Opt. Express* **2020**, *28*, 5147. [CrossRef]
30. Paesani, S.; Borghi, M.; Signorini, S.; Maïnos, A.; Pavesi, L.; Laing, A. Near-ideal spontaneous photon sources in silicon quantum photonics. *Nat. Commun.* **2020**, *11*, 2505. [CrossRef]
31. Shukhin, A.A.; Keloth, J.; Hakuta, K.; Kalachev, A.A. Heralded single-photon and correlated-photon-pair generation via spontaneous four-wave mixing in tapered optical fibers. *Phys. Rev. A* **2020**, *101*, 053822. [CrossRef]
32. Signorini, S.; Sanna, M.; Piccione, S.; Ghulinyan, M.; Tidemand-Lichtenberg, P.; Pedersen, C.; Pavesi, L. A silicon source of heralded single photons at 2 micrometers. *APL Photonics* **2021**, *6*, 126103. [CrossRef]
33. Tang, J.; Tang, L.; Wu, H.; Wu, Y.; Sun, H.; Zhang, H.; Li, T.; Lu, Y.; Xiao, M.; Xia, K. Towards On-Demand Heralded Single-Photon Sources via Photon Blockade. *Phys. Rev. Appl.* **2021**, *15*, 064020. [CrossRef]
34. Davis, S.I.; Mueller, A.; Valivarthi, R.; Lauk, N.; Narvaez, L.; Korzh, B.; Beyer, A.D.; Cerri, O.; Colangelo, M.; Berggren, K.K.; et al. Improved Heralded Single-Photon Source with a Photon-Number-Resolving Superconducting Nanowire Detector. *Phys. Rev. Appl.* **2022**, *18*, 064007. [CrossRef]
35. Stasi, L.; Caspar, P.; Brydges, T.; Zbinden, H.; Bussières, F.; Thew, R. High-efficiency photon-number-resolving detector for improving heralded single-photon sources. *Quant. Sci. Technol.* **2023**, *8*, 045006. [CrossRef]
36. Wang, H.; Yuan, H.; Zeng, Q.; Zhou, L.; Ma, H.; Yuan, Z. Bright Heralded Single-Photon Source with Ideal Purity. *arXiv* **2024**, arXiv:2404.03236.
37. Pittman, T.B.; Jacobs, B.C.; Franson, J.D. Single photons on pseudodemand from stored parametric down-conversion. *Phys. Rev. A* **2002**, *66*, 042303. [CrossRef]
38. Migdall, A.L.; Branning, D.; Castelletto, S. Tailoring single-photon and multiphoton probabilities of a single-photon on-demand source. *Phys. Rev. A* **2002**, *66*, 053805. [CrossRef]
39. Jeffrey, E.; Peters, N.A.; Kwiat, P.G. Towards a periodic deterministic source of arbitrary single-photon states. *New J. Phys.* **2004**, *6*, 100. [CrossRef]
40. Mower, J.; Englund, D. Efficient generation of single and entangled photons on a silicon photonic integrated chip. *Phys. Rev. A* **2011**, *84*, 052326. [CrossRef]
41. Mazzarella, L.; Ticozzi, F.; Sergienko, A.V.; Vallone, G.; Villoresi, P. Asymmetric architecture for heralded single-photon sources. *Phys. Rev. A* **2013**, *88*, 023848. [CrossRef]
42. Adam, P.; Mechler, M.; Santa, I.; Koniorczyk, M. Optimization of periodic single-photon sources. *Phys. Rev. A* **2014**, *90*, 053834. [CrossRef]
43. Francis-Jones, R.J.A.; Mosley, P.J. Exploring the limits of multiplexed photon-pair sources for the preparation of pure single-photon states. *arXiv* **2014**, arXiv:1409.1394.
44. Schmiegelow, C.T.; Larotonda, M.A. Multiplexing photons with a binary division strategy. *Appl. Phys. B* **2014**, *116*, 447–454. [CrossRef]
45. Bonneau, D.; Mendoza, G.J.; O'Brien, J.L.; Thompson, M.G. Effect of loss on multiplexed single-photon sources. *New J. Phys.* **2015**, *17*, 043057. [CrossRef]
46. Francis-Jones, R.J.A.; Mosley, P.J. Temporal Loop Multiplexing: A resource efficient scheme for multiplexed photon-pair sources. *arXiv* **2015**, arXiv:1503.06178.
47. Rohde, P.P.; Helt, L.G.; Steel, M.J.; Gilchrist, A. Multiplexed single-photon-state preparation using a fiber-loop architecture. *Phys. Rev. A* **2015**, *92*, 053829. [CrossRef]
48. Bodog, F.; Adam, P.; Mechler, M.; Santa, I.; Koniorczyk, M. Optimization of periodic single-photon sources based on combined multiplexing. *Phys. Rev. A* **2016**, *94*, 033853. [CrossRef]
49. Heuck, M.; Pant, M.; Englund, D.R. Temporally and spectrally multiplexed single photon source using quantum feedback control for scalable photonic quantum technologies. *New J. Phys.* **2018**, *20*, 063046. [CrossRef]
50. Bodog, F.; Mechler, M.; Koniorczyk, M.; Adam, P. Optimization of multiplexed single-photon sources operated with photon-number-resolving detectors. *Phys. Rev. A* **2020**, *102*, 013513. [CrossRef]
51. Magnoni, A.G.; Knoll, L.T.; Larotonda, M.A. Scheme for sub-shot-noise transmission measurement using a time-multiplexed single-photon source. *J. Opt. Soc. Am. B* **2021**, *38*, 2502. [CrossRef]

52. Adam, P.; Bodog, F.; Koniorczyk, M.; Mechler, M. Single-photon sources based on asymmetric spatial multiplexing with optimized inputs. *Phys. Rev. A* **2022**, *105*, 063721. [CrossRef]
53. Adam, P.; Bodog, F.; Mechler, M. Spatially multiplexed single-photon sources based on incomplete binary-tree multiplexers. *Opt. Express* **2022**, *30*, 6999. [CrossRef] [PubMed]
54. Adam, P.; Mechler, M. Single-photon sources based on incomplete binary-tree multiplexers with optimal structure. *Opt. Express* **2023**, *31*, 30194. [CrossRef]
55. Adam, P.; Mechler, M. Single-photon sources based on stepwise optimized binary-tree multiplexers. *Opt. Express* **2024**, *32*, 17173. [CrossRef]
56. Adam, P.; Mechler, M. Single-photon sources based on incomplete binary-tree multiplexers with optimized inputs. *Phys. Lett. A* **2024**, *503*, 129416. [CrossRef]
57. Adam, P.; Mechler, M. Reducing Multiphoton Noise in Multiplexed Single-Photon Sources. *Photonics* **2024**, *11*, 728. [CrossRef]
58. Ma, X.s.; Zotter, S.; Kofler, J.; Jennewein, T.; Zeilinger, A. Experimental generation of single photons via active multiplexing. *Phys. Rev. A* **2011**, *83*, 043814. [CrossRef]
59. Collins, M.; Xiong, C.; Rey, I.; Vo, T.; He, J.; Shahnia, S.; Reardon, C.; Krauss, T.; Steel, M.; Clark, A.; et al. Integrated spatial multiplexing of heralded single-photon sources. *Nat. Commun.* **2013**, *4*, 2582. [CrossRef]
60. Xiong, C.; Vo, T.D.; Collins, M.J.; Li, J.; Krauss, T.F.; Steel, M.J.; Clark, A.S.; Eggleton, B.J. Bidirectional multiplexing of heralded single photons from a silicon chip. *Opt. Lett.* **2013**, *38*, 5176. [CrossRef]
61. Meany, T.; Ngah, L.A.; Collins, M.J.; Clark, A.S.; Williams, R.J.; Eggleton, B.J.; Steel, M.J.; Withford, M.J.; Alibart, O.; Tanzilli, S. Hybrid photonic circuit for multiplexed heralded single photons. *Laser Photonics Rev.* **2014**, *8*, L42–L46. [CrossRef]
62. Kaneda, F.; Christensen, B.G.; Wong, J.J.; Park, H.S.; McCusker, K.T.; Kwiat, P.G. Time-multiplexed heralded single-photon source. *Optica* **2015**, *2*, 1010. [CrossRef]
63. Francis-Jones, R.J.A.; Hoggarth, R.A.; Mosley, P.J. All-fiber multiplexed source of high-purity single photons. *Optica* **2016**, *3*, 1270. [CrossRef]
64. Kiyohara, T.; Okamoto, R.; Takeuchi, S. Realization of multiplexing of heralded single photon sources using photon number resolving detectors. *Opt. Express* **2016**, *24*, 27288. [CrossRef]
65. Mendoza, G.J.; Santagati, R.; Munns, J.; Hemsley, E.; Piekarek, M.; Martín-López, E.; Marshall, G.D.; Bonneau, D.; Thompson, M.G.; O'Brien, J.L. Active temporal and spatial multiplexing of photons. *Optica* **2016**, *3*, 127. [CrossRef]
66. Xiong, C.; Zhang, X.; Liu, Z.; Collins, M.J.; Mahendra, A.; Helt, L.G.; Steel, M.J.; Choi, D.Y.; Chae, C.J.; Leong, P.H.W.; et al. Active temporal multiplexing of indistinguishable heralded single photons. *Nat. Commun.* **2016**, *7*, 10853. [CrossRef]
67. Hoggarth, R.A.; Francis-Jones, R.J.A.; Mosley, P.J. Resource-efficient fibre-integrated temporal multiplexing of heralded single photons. *J. Opt.* **2017**, *19*, 125503. [CrossRef]
68. Grimau Puigibert, M.; Aguilar, G.; Zhou, Q.; Marsili, F.; Shaw, M.; Verma, V.; Nam, S.; Oblak, D.; Tittel, W. Heralded Single Photons Based on Spectral Multiplexing and Feed-Forward Control. *Phys. Rev. Lett.* **2017**, *119*, 083601. [CrossRef]
69. Joshi, C.; Farsi, A.; Clemmen, S.; Ramelow, S.; Gaeta, A.L. Frequency multiplexing for quasi-deterministic heralded single-photon sources. *Nat. Commun.* **2018**, *9*, 847. [CrossRef] [PubMed]
70. Kaneda, F.; Kwiat, P.G. High-efficiency single-photon generation via large-scale active time multiplexing. *Sci. Adv.* **2019**, *5*. [CrossRef]
71. Hiemstra, T.; Parker, T.; Humphreys, P.; Tiedau, J.; Beck, M.; Karpiński, M.; Smith, B.; Eckstein, A.; Kolthammer, W.; Walmsley, I. Pure Single Photons From Scalable Frequency Multiplexing. *Phys. Rev. Appl.* **2020**, *14*, 014052. [CrossRef]
72. Yu, H.; Yuan, C.; Zhang, R.; Zhang, Z.; Li, H.; Wang, Y.; Deng, G.; You, L.; Song, H.; Wang, Z.; et al. Spectrally multiplexed indistinguishable single-photon generation at telecom-band. *Photon. Res.* **2022**, *10*, 1417. [CrossRef]
73. Fasel, S.; Alibart, O.; Tanzilli, S.; Baldi, P.; Beveratos, A.; Gisin, N.; Zbinden, H. High-quality asynchronous heralded single-photon source at telecom wavelength. *New J. Phys.* **2004**, *6*, 163. [CrossRef]
74. Baek, S.Y.; Kwon, O.; Kim, Y.H. Temporal shaping of a heralded single-photon wave packet. *Phys. Rev. A* **2008**, *77*, 013829. [CrossRef]
75. Castelletto, S.A.; Scholten, R.E. Heralded single photon sources: A route towards quantum communication technology and photon standards. *Eur. Phys. J. Appl. Phys.* **2008**, *41*, 181–194. [CrossRef]
76. Montaut, N.; Sansoni, L.; Meyer-Scott, E.; Ricken, R.; Quiring, V.; Herrmann, H.; Silberhorn, C. High-Efficiency Plug-and-Play Source of Heralded Single Photons. *Phys. Rev. Appl.* **2017**, *8*, 024021. [CrossRef]
77. Avenhaus, M.; Coldenstrodt-Ronge, H.B.; Laiho, K.; Mauerer, W.; Walmsley, I.A.; Silberhorn, C. Photon Number Statistics of Multimode Parametric Down-Conversion. *Phys. Rev. Lett.* **2008**, *101*, 053601. [CrossRef]
78. Mauerer, W.; Avenhaus, M.; Helwig, W.; Silberhorn, C. How colors influence numbers: Photon statistics of parametric down-conversion. *Phys. Rev. A* **2009**, *80*, 053815. [CrossRef]
79. Takesue, H.; Shimizu, K. Effects of multiple pairs on visibility measurements of entangled photons generated by spontaneous parametric processes. *Opt. Commun.* **2010**, *283*, 276–287. [CrossRef]
80. Almeida, A.J.; Silva, N.A.; Andre, P.S.; Pinto, A.N. Four-wave mixing: Photon statistics and the impact on a co-propagating quantum signal. *Opt. Commun.* **2012**, *285*, 2956–2960. [CrossRef]
81. Harder, G.; Bartley, T.J.; Lita, A.E.; Nam, S.W.; Gerrits, T.; Silberhorn, C. Single-Mode Parametric-Down-Conversion States with 50 Photons as a Source for Mesoscopic Quantum Optics. *Phys. Rev. Lett.* **2016**, *116*, 143601. [CrossRef]

82. Christ, A.; Silberhorn, C. Limits on the deterministic creation of pure single-photon states using parametric down-conversion. *Phys. Rev. A* **2012**, *85*, 023829. [CrossRef]
83. Paul, H.; Törmä, P.; Kiss, T.; Jex, I. Photon Chopping: New Way to Measure the Quantum State of Light. *Phys. Rev. Lett.* **1996**, *76*, 2464–2467. [CrossRef] [PubMed]
84. Paul, H.; Törmä, P.; Kiss, T.; Jex, I. Multiple coincidences and the quantum state reconstruction problem. *Phys. Rev. A* **1997**, *56*, 4076–4085. [CrossRef]
85. Řeháček, J.; Hradil, Z.; Haderka, O.; Peřina, J.; Hamar, M. Multiple-photon resolving fiber-loop detector. *Phys. Rev. A* **2003**, *67*, 061801. [CrossRef]
86. Fitch, M.J.; Jacobs, B.C.; Pittman, T.B.; Franson, J.D. Photon-number resolution using time-multiplexed single-photon detectors. *Phys. Rev. A* **2003**, *68*, 043814. [CrossRef]
87. Achilles, D.; Silberhorn, C.; Śliwa, C.; Banaszek, K.; Walmsley, I.A. Fiber-assisted detection with photon number resolution. *Opt. Lett.* **2003**, *28*, 2387. [CrossRef]
88. Achilles, D.; Silberhorn, C.; Sliwa, C.; Banaszek, K.; Walmsley, I.A.; Fitch, M.J.; Jacobs, B.C.; Pittman, T.B.; Franson, J.D. Photon-number-resolving detection using time-multiplexing. *J. Mod. Opt.* **2004**, *51*, 1499–1515. [CrossRef]
89. Afek, I.; Natan, A.; Ambar, O.; Silberberg, Y. Quantum state measurements using multipixel photon detectors. *Phys. Rev. A* **2009**, *79*, 043830. [CrossRef]
90. Sperling, J.; Vogel, W.; Agarwal, G.S. True photocounting statistics of multiple on-off detectors. *Phys. Rev. A* **2012**, *85*, 023820. [CrossRef]
91. Natarajan, C.M.; Zhang, L.; Coldenstrodt-Ronge, H.; Donati, G.; Dorenbos, S.N.; Zwiller, V.; Walmsley, I.A.; Hadfield, R.H. Quantum detector tomography of a time-multiplexed superconducting nanowire single-photon detector at telecom wavelengths. *Opt. Express* **2013**, *21*, 893. [CrossRef] [PubMed]
92. Helt, L.G.; Steel, M.J. Effect of dark counts on single-photon heralding with quasi-number-resolving detection schemes. *Opt. Lett.* **2017**, *42*, 4792. [CrossRef] [PubMed]
93. Kruse, R.; Tiedau, J.; Bartley, T.J.; Barkhofen, S.; Silberhorn, C. Limits of the time-multiplexed photon-counting method. *Phys. Rev. A* **2017**, *95*, 023815. [CrossRef]
94. Chen, X.; Ding, C.; Pan, H.; Huang, K.; Laurat, J.; Wu, G.; Wu, E. Temporal and spatial multiplexed infrared single-photon counter based on high-speed avalanche photodiode. *Sci. Rep.* **2017**, *7*, 44600. [CrossRef] [PubMed]
95. Jönsson, M.; Björk, G. Evaluating the performance of photon-number-resolving detectors. *Phys. Rev. A* **2019**, *99*, 043822. [CrossRef]
96. Jönsson, M.; Björk, G. Photon-counting distribution for arrays of single-photon detectors. *Phys. Rev. A* **2020**, *101*, 013815. [CrossRef]
97. Nehra, R.; Chang, C.H.; Yu, Q.; Beling, A.; Pfister, O. Photon-number-resolving segmented detectors based on single-photon avalanche-photodiodes. *Opt. Express* **2020**, *28*, 3660. [CrossRef]
98. Steinhauer, S.; Gyger, S.; Zwiller, V. Progress on large-scale superconducting nanowire single-photon detectors. *Appl. Phys. Lett.* **2021**, *118*. [CrossRef]
99. Hao, H.; Zhao, Q.Y.; Huang, Y.H.; Deng, J.; Yang, F.; Ru, S.Y.; Liu, Z.; Wan, C.; Liu, H.; Li, Z.J.; et al. A compact multi-pixel superconducting nanowire single-photon detector array supporting gigabit space-to-ground communications. *Light Sci. Appl.* **2024**, *13*, 25. [CrossRef]
100. Divochiy, A.; Marsili, F.; Bitauld, D.; Gaggero, A.; Leoni, R.; Mattioli, F.; Korneev, A.; Seleznev, V.; Kaurova, N.; Minaeva, O.; et al. Superconducting nanowire photon-number-resolving detector at telecommunication wavelengths. *Nat. Photonics* **2008**, *2*, 302–306. [CrossRef]
101. Jahanmirinejad, S.; Frucci, G.; Mattioli, F.; Sahin, D.; Gaggero, A.; Leoni, R.; Fiore, A. Photon-number resolving detector based on a series array of superconducting nanowires. *Appl. Phys. Lett.* **2012**, *101*, 072602. [CrossRef]
102. Zhou, Z.; Jahanmirinejad, S.; Mattioli, F.; Sahin, D.; Frucci, G.; Gaggero, A.; Leoni, R.; Fiore, A. Superconducting series nanowire detector counting up to twelve photons. *Opt. Express* **2014**, *22*, 3475. [CrossRef] [PubMed]
103. Mattioli, F.; Zhou, Z.; Gaggero, A.; Gaudio, R.; Jahanmirinejad, S.; Sahin, D.; Marsili, F.; Leoni, R.; Fiore, A. Photon-number-resolving superconducting nanowire detectors. *Supercond. Sci. Technol.* **2015**, *28*, 104001. [CrossRef]
104. Zhang, W.; Huang, J.; Zhang, C.; You, L.; Lv, C.; Zhang, L.; Li, H.; Wang, Z.; Xie, X. A 16-Pixel Interleaved Superconducting Nanowire Single-Photon Detector Array with a Maximum Count Rate Exceeding 1.5 GHz. *IEEE Trans. Appl. Supercond.* **2019**, *29*, 2200204. [CrossRef]
105. Mattioli, F.; Zhou, Z.; Gaggero, A.; Gaudio, R.; Leoni, R.; Fiore, A. Photon-counting and analog operation of a 24-pixel photon number resolving detector based on superconducting nanowires. *Opt. Express* **2016**, *24*, 9067. [CrossRef]
106. Kardynał, B.E.; Yuan, Z.L.; Shields, A.J. An avalanche-photodiode-based photon-number-resolving detector. *Nat. Photonics* **2008**, *2*, 425–428. [CrossRef]
107. Thomas, O.; Yuan, Z.L.; Dynes, J.F.; Sharpe, A.W.; Shields, A.J. Efficient photon number detection with silicon avalanche photodiodes. *Appl. Phys. Lett.* **2010**, *97*, 31102. [CrossRef]
108. Gansen, E.J.; Rowe, M.A.; Greene, M.B.; Rosenberg, D.; Harvey, T.E.; Su, M.Y.; Hadfield, R.H.; Nam, S.W.; Mirin, R.P. Photon-number-discriminating detection using a quantum-dot, optically gated, field-effect transistor. *Nat. Photonics* **2007**, *1*, 585–588. [CrossRef]

109. Kardynał, B.E.; Hees, S.S.; Shields, A.J.; Nicoll, C.; Farrer, I.; Ritchie, D.A. Photon number resolving detector based on a quantum dot field effect transistor. *Appl. Phys. Lett.* **2007**, *90*, 181114. [CrossRef]
110. Cahall, C.; Nicolich, K.L.; Islam, N.T.; Lafyatis, G.P.; Miller, A.J.; Gauthier, D.J.; Kim, J. Multi-photon detection using a conventional superconducting nanowire single-photon detector. *Optica* **2017**, *4*, 1534. [CrossRef]
111. Lita, A.E.; Reddy, D.V.; Verma, V.B.; Mirin, R.P.; Nam, S.W. Development of Superconducting Single-Photon and Photon-Number Resolving Detectors for Quantum Applications. *J. Light. Technol.* **2022**, *40*, 7578–7597. [CrossRef]
112. Cabrera, B.; Clarke, R.M.; Colling, P.; Miller, A.J.; Nam, S.; Romani, R.W. Detection of single infrared, optical, and ultraviolet photons using superconducting transition edge sensors. *Appl. Phys. Lett.* **1998**, *73*, 735–737. [CrossRef]
113. Miller, A.J.; Nam, S.W.; Martinis, J.M.; Sergienko, A.V. Demonstration of a low-noise near-infrared photon counter with multiphoton discrimination. *Appl. Phys. Lett.* **2003**, *83*, 791–793. [CrossRef]
114. Rosenberg, D.; Lita, A.; Miller, A.; Nam, S. Noise-free high-efficiency photon-number-resolving detectors. *Phys. Rev. A* **2005**, *71*, 061803. [CrossRef]
115. Rosenberg, D.; Lita, A.; Miller, A.; Nam, S.; Schwall, R. Performance of photon-number resolving transition-edge sensors with integrated 1550 nm resonant cavities. *IEEE Trans. Appl. Supercond.* **2005**, *15*, 575–578. [CrossRef]
116. Lita, A.E.; Miller, A.J.; Nam, S.W. Counting near-infrared single-photons with 95% efficiency. *Opt. Express* **2008**, *16*, 3032. [CrossRef]
117. Lita, A.E.; Calkins, B.; Pellochoud, L.A.; Miller, A.J.; Nam, S. High-Efficiency Photon-Number-Resolving Detectors based on Hafnium Transition-Edge Sensors. *AIP Conf. Proc.* **2009**, *1185*, 351–354 [CrossRef]
118. Lita, A.E.; Calkins, B.; Pellouchoud, L.A.; Miller, A.J.; Nam, S. Superconducting transition-edge sensors optimized for high-efficiency photon-number resolving detectors. In *Advanced Photon Counting Techniques IV, Proceedings of the SPIE Defense, Security, and Sensing, Orlando, FL, USA, 5–9 April 2010*; Itzler, M.A., Campbell, J.C., Eds.; SPIE: Bellingham, WA, USA, 2010; Volume 7681, p. 76810D. [CrossRef]
119. Fukuda, D.; Fujii, G.; Numata, T.; Amemiya, K.; Yoshizawa, A.; Tsuchida, H.; Fujino, H.; Ishii, H.; Itatani, T.; Inoue, S.; et al. Titanium-based transition-edge photon number resolving detector with 98% detection efficiency with index-matched small-gap fiber coupling. *Opt. Express* **2011**, *19*, 870. [CrossRef]
120. Schmidt, M.; von Helversen, M.; López, M.; Gericke, F.; Schlottmann, E.; Heindel, T.; Kück, S.; Reitzenstein, S.; Beyer, J. Photon-Number-Resolving Transition-Edge Sensors for the Metrology of Quantum Light Sources. *J. Low Temp. Phys.* **2018**, *193*, 1243–1250. [CrossRef]
121. Fukuda, D. Single-Photon Measurement Techniques with a Superconducting Transition Edge Sensor. *IEICE Trans. Electron.* **2019**, *E102.C*, 230–234. [CrossRef]
122. Kaneda, F.; Xu, F.; Chapman, J.; Kwiat, P.G. Quantum-memory-assisted multi-photon generation for efficient quantum information processing. *Optica* **2017**, *4*, 1034. [CrossRef]
123. Brandhofer, S.; Myers, C.R.; Devitt, S.; Polian, I. Multiplexed pseudo-deterministic photon source with asymmetric switching elements. *Res. Dir. Quantum Technol.* **2024**, *2*, e3. [CrossRef]
124. Gimeno-Segovia, M.; Cable, H.; Mendoza, G.J.; Shadbolt, P.; Silverstone, J.W.; Carolan, J.; Thompson, M.G.; O'Brien, J.L.; Rudolph, T. Relative multiplexing for minimising switching in linear-optical quantum computing. *New J. Phys.* **2017**, *19*, 063013. [CrossRef]
125. Zhang, X.; Lee, Y.H.; Bell, B.A.; Leong, P.H.W.; Rudolph, T.; Eggleton, B.J.; Xiong, C. Indistinguishable heralded single photon generation via relative temporal multiplexing of two sources. *Opt. Express* **2017**, *25*, 26067. [CrossRef] [PubMed]
126. Lee, E.; Lee, S.M.; Park, H.S. Relative time multiplexing of heralded telecom-band single-photon sources using switchable optical fiber delays. *Opt. Express* **2019**, *27*, 24545. [CrossRef] [PubMed]
127. Magnoni, A.G.; López Grande, I.H.; Knoll, L.T.; Larotonda, M.A. Performance of a temporally multiplexed single-photon source with imperfect devices. *Quantum Inf. Process.* **2019**, *18*, 311. [CrossRef]
128. Peters, N.A.; Arnold, K.J.; VanDevender, A.P.; Jeffrey, E.R.; Rangarajan, R.; Hosten, O.; Barreiro, J.T.; Altepeter, J.B.; Kwiat, P.G. Towards a quasi-deterministic single-photon source. In *Quantum Communications and Quantum Imaging IV, Proceedings of the SPIE Optics + Photonics, San Diego, CA, USA, 13–17 August 2006*; Meyers, R.E., Shih, Y., Deacon, K.S., Eds.; SPIE: Bellingham, WA, USA, 2006; Volume 6305, p. 630507. [CrossRef]
129. Loredo, J.C.; Zakaria, N.A.; Somaschi, N.; Anton, C.; de Santis, L.; Giesz, V.; Grange, T.; Broome, M.A.; Gazzano, O.; Coppola, G.; et al. Scalable performance in solid-state single-photon sources. *Optica* **2016**, *3*, 433. [CrossRef]
130. Wang, H.; He, Y.; Li, Y.H.; Su, Z.E.; Li, B.; Huang, H.L.; Ding, X.; Chen, M.C.; Liu, C.; Qin, J.; et al. High-efficiency multiphoton boson sampling. *Nat. Photonics* **2017**, *11*, 361–365. [CrossRef]
131. Senellart, P.; Solomon, G.; White, A. High-performance semiconductor quantum-dot single-photon sources. *Nat. Nanotechnol.* **2017**, *12*, 1026–1039. [CrossRef]
132. Thomas, S.; Senellart, P. The race for the ideal single-photon source is on. *Nat. Nanotechnol.* **2021**, *16*, 367–368. [CrossRef]
133. Tomm, N.; Javadi, A.; Antoniadis, N.O.; Najer, D.; Löbl, M.C.; Korsch, A.R.; Schott, R.; Valentin, S.R.; Wieck, A.D.; Ludwig, A.; et al. A bright and fast source of coherent single photons. *Nat. Nanotechnol.* **2021**, *16*, 399–403. [CrossRef] [PubMed]
134. Adcock, J.C.; Bacco, D.; Ding, Y. Enhancement of a silicon waveguide single photon source by temporal multiplexing. *Quantum Sci. Technol.* **2022**, *7*, 025025. [CrossRef]
135. Magnoni, A.G.; Knoll, L.T.; Wölcken, L.; Defant, J.; Morales, J.; Larotonda, M.A. Toward an optical-fiber-based temporally multiplexed single-photon source. *Phys. Rev. A* **2024**, *110*, 033712. [CrossRef]

136. Scarani, V.; Bechmann-Pasquinucci, H.; Cerf, N.J.; Dušek, M.; Lütkenhaus, N.; Peev, M. The security of practical quantum key distribution. *Rev. Mod. Phys.* **2009**, *81*, 1301–1350. [CrossRef]
137. Lo, H.K.; Curty, M.; Tamaki, K. Secure quantum key distribution. *Nat. Photonics* **2014**, *8*, 595–604. [CrossRef]
138. Moskovich, D. An Overview of the State of the Art for Practical Quantum Key Distribution. *arXiv* **2015**, arXiv:1504.05471.
139. Diamanti, E.; Lo, H.K.; Qi, B.; Yuan, Z. Practical challenges in quantum key distribution. *npj Quantum Inf.* **2016**, *2*, 16025. [CrossRef]
140. Abushgra, A.A. Variations of QKD Protocols Based on Conventional System Measurements: A Literature Review. *Cryptography* **2022**, *6*, 12. [CrossRef]
141. Cao, Y.; Zhao, Y.; Wang, Q.; Zhang, J.; Ng, S.X.; Hanzo, L. The Evolution of Quantum Key Distribution Networks: On the Road to the Qinternet. *IEEE Commun. Surv. Tutorials* **2022**, *24*, 839–894. [CrossRef]
142. Bennett, C.H.; Brassard, G. Quantum cryptography: Public key distribution and coin tossing. *Theor. Comp. Sci.* **2014**, *560*, 7–11. [CrossRef]
143. Peev, M.; Pacher, C.; Alléaume, R.; Barreiro, C.; Bouda, J.; Boxleitner, W.; Debuisschert, T.; Diamanti, E.; Dianati, M.; Dynes, J.F.; et al. The SECOQC quantum key distribution network in Vienna. *New J. Phys.* **2009**, *11*, 075001. [CrossRef]
144. Sasaki, M.; Fujiwara, M.; Ishizuka, H.; Klaus, W.; Wakui, K.; Takeoka, M.; Miki, S.; Yamashita, T.; Wang, Z.; Tanaka, A.; et al. Field test of quantum key distribution in the Tokyo QKD Network. *Opt. Express* **2011**, *19*, 10387. [CrossRef] [PubMed]
145. Yin, H.L.; Chen, T.Y.; Yu, Z.W.; Liu, H.; You, L.X.; Zhou, Y.H.; Chen, S.J.; Mao, Y.; Huang, M.Q.; Zhang, W.J.; et al. Measurement-Device-Independent Quantum Key Distribution Over a 404 km Optical Fiber. *Phys. Rev. Lett.* **2016**, *117*, 190501. [CrossRef] [PubMed]
146. Chen, J.P.; Zhang, C.; Liu, Y.; Jiang, C.; Zhang, W.J.; Han, Z.Y.; Ma, S.Z.; Hu, X.L.; Li, Y.H.; Liu, H.; et al. Twin-field quantum key distribution over a 511 km optical fibre linking two distant metropolitan areas. *Nat. Photonics* **2021**, *15*, 570–575. [CrossRef]
147. Liu, H.; Jiang, C.; Zhu, H.T.; Zou, M.; Yu, Z.W.; Hu, X.L.; Xu, H.; Ma, S.; Han, Z.; Chen, J.P.; et al. Field Test of Twin-Field Quantum Key Distribution through Sending-or-Not-Sending over 428 km. *Phys. Rev. Lett.* **2021**, *126*, 250502. [CrossRef]
148. Schiavon, M.; Vallone, G.; Ticozzi, F.; Villoresi, P. Heralded single-photon sources for quantum-key-distribution applications. *Phys. Rev. A* **2016**, *93*, 012331. [CrossRef]
149. Bennett, C.H.; Brassard, G.; Crépeau, C.; Jozsa, R.; Peres, A.; Wootters, W.K. Teleporting an unknown quantum state via dual classical and Einstein-Podolsky-Rosen channels. *Phys. Rev. Lett.* **1993**, *70*, 1895–1899. [CrossRef]
150. Pirandola, S.; Eisert, J.; Weedbrook, C.; Furusawa, A.; Braunstein, S.L. Advances in quantum teleportation. *Nat. Photonics* **2015**, *9*, 641–652. [CrossRef]
151. Ursin, R.; Jennewein, T.; Aspelmeyer, M.; Kaltenbaek, R.; Lindenthal, M.; Walther, P.; Zeilinger, A. Quantum teleportation across the Danube. *Nature* **2004**, *430*, 849. [CrossRef]
152. Landry, O.; van Houwelingen, J.A.W.; Beveratos, A.; Zbinden, H.; Gisin, N. Quantum teleportation over the Swisscom telecommunication network. *J. Opt. Soc. Am. B* **2007**, *24*, 398. [CrossRef]
153. Ma, X.S.; Herbst, T.; Scheidl, T.; Wang, D.; Kropatschek, S.; Naylor, W.; Wittmann, B.; Mech, A.; Kofler, J.; Anisimova, E.; et al. Quantum teleportation over 143 kilometres using active feed-forward. *Nature* **2012**, *489*, 269–273. [CrossRef] [PubMed]
154. Yin, J.; Ren, J.G.; Lu, H.; Cao, Y.; Yong, H.L.; Wu, Y.P.; Liu, C.; Liao, S.K.; Zhou, F.; Jiang, Y.; et al. Quantum teleportation and entanglement distribution over 100-kilometre free-space channels. *Nature* **2012**, *488*, 185–188. [CrossRef] [PubMed]
155. Wang, X.L.; Cai, X.D.; Su, Z.E.; Chen, M.C.; Wu, D.; Li, L.; Liu, N.L.; Lu, C.Y.; Pan, J.W. Quantum teleportation of multiple degrees of freedom of a single photon. *Nature* **2015**, *518*, 516–519. [CrossRef] [PubMed]
156. Takesue, H.; Dyer, S.D.; Stevens, M.J.; Verma, V.; Mirin, R.P.; Nam, S.W. Quantum teleportation over 100 km of fiber using highly efficient superconducting nanowire single-photon detectors. *Optica* **2015**, *2*, 832. [CrossRef]
157. Knill, E.; Laflamme, R.; Milburn, G.J. A scheme for efficient quantum computation with linear optics. *Nature* **2001**, *409*, 46–52. [CrossRef]
158. Jennewein, T.; Barbieri, M.; White, A.G. Single-photon device requirements for operating linear optics quantum computing outside the post-selection basis. *J. Mod. Opt.* **2011**, *58*, 276–287. [CrossRef]
159. Raussendorf, R.; Briegel, H.J. A One-Way Quantum Computer. *Phys. Rev. Lett.* **2001**, *86*, 5188–5191. [CrossRef]
160. Raussendorf, R.; Browne, D.E.; Briegel, H.J. Measurement-based quantum computation on cluster states. *Phys. Rev. A* **2003**, *68*, 022312. [CrossRef]
161. Nielsen, M.A. Optical Quantum Computation Using Cluster States. *Phys. Rev. Lett.* **2004**, *93*, 040503. [CrossRef]
162. Rudolph, T. Why I am optimistic about the silicon-photonic route to quantum computing. *APL Photonics* **2017**, *2*, 030901. [CrossRef]
163. Kiesel, N.; Schmid, C.; Weber, U.; Tóth, G.; Gühne, O.; Ursin, R.; Weinfurter, H. Experimental Analysis of a Four-Qubit Photon Cluster State. *Phys. Rev. Lett.* **2005**, *95*, 210502. [CrossRef] [PubMed]
164. Walther, P.; Resch, K.J.; Rudolph, T.; Schenck, E.; Weinfurter, H.; Vedral, V.; Aspelmeyer, M.; Zeilinger, A. Experimental one-way quantum computing. *Nature* **2005**, *434*, 169–176. [CrossRef] [PubMed]
165. Schmid, C.; Kiesel, N.; Wieczorek, W.; Weinfurter, H. The entanglement of the four-photon cluster state. *New J. Phys.* **2007**, *9*, 236. [CrossRef]
166. Ciampini, M.A.; Orieux, A.; Paesani, S.; Sciarrino, F.; Corrielli, G.; Crespi, A.; Ramponi, R.; Osellame, R.; Mataloni, P. Path-polarization hyperentangled and cluster states of photons on a chip. *Light Sci. Appl.* **2016**, *5*, e16064. [CrossRef] [PubMed]

167. Adcock, J.C.; Vigliar, C.; Santagati, R.; Silverstone, J.W.; Thompson, M.G. Programmable four-photon graph states on a silicon chip. *Nat. Commun.* **2019**, *10*, 3528. [CrossRef]
168. Meyer-Scott, E.; Prasannan, N.; Dhand, I.; Eigner, C.; Quiring, V.; Barkhofen, S.; Brecht, B.; Plenio, M.B.; Silberhorn, C. Scalable Generation of Multiphoton Entangled States by Active Feed-Forward and Multiplexing. *Phys. Rev. Lett.* **2022**, *129*, 150501. [CrossRef]
169. Fattal, D.; Inoue, K.; Vučković, J.; Santori, C.; Solomon, G.S.; Yamamoto, Y. Entanglement Formation and Violation of Bell's Inequality with a Semiconductor Single Photon Source. *Phys. Rev. Lett.* **2004**, *92*, 037903. [CrossRef]
170. Varnava, M.; Browne, D.E.; Rudolph, T. How Good Must Single Photon Sources and Detectors Be for Efficient Linear Optical Quantum Computation? *Phys. Rev. Lett.* **2008**, *100*, 060502. [CrossRef] [PubMed]
171. Zhang, Q.; Bao, X.H.; Lu, C.Y.; Zhou, X.Q.; Yang, T.; Rudolph, T.; Pan, J.W. Demonstration of a scheme for the generation of "event-ready" entangled photon pairs from a single-photon source. *Phys. Rev. A* **2008**, *77*, 062316. [CrossRef]
172. Zhang, S.; Dong, Y.; Zou, X.; Shi, B.; Guo, G. Continuous-variable-entanglement distillation with photon addition. *Phys. Rev. A* **2013**, *88*, 032324. [CrossRef]
173. Li, J.P.; Qin, J.; Chen, A.; Duan, Z.C.; Yu, Y.; Huo, Y.; Höfling, S.; Lu, C.Y.; Chen, K.; Pan, J.W. Multiphoton Graph States from a Solid-State Single-Photon Source. *ACS Photonics* **2020**, *7*, 1603–1610. [CrossRef]
174. Lund, A.P.; Bremner, M.J.; Ralph, T.C. Quantum sampling problems, Boson Sampling and quantum supremacy. *npj Quantum Inf.* **2017**, *3*, 15. [CrossRef]
175. Bentivegna, M.; Spagnolo, N.; Vitelli, C.; Flamini, F.; Viggianiello, N.; Latmiral, L.; Mataloni, P.; Brod, D.J.; Galvão, E.F.; Crespi, A.; et al. Experimental scattershot boson sampling. *Sci. Adv.* **2015**, *1*. [CrossRef] [PubMed]
176. He, Y.; Ding, X.; Su, Z.E.; Huang, H.L.; Qin, J.; Wang, C.; Unsleber, S.; Chen, C.; Wang, H.; He, Y.M.; et al. Time-Bin-Encoded Boson Sampling with a Single-Photon Device. *Phys. Rev. Lett.* **2017**, *118*, 190501. [CrossRef]
177. Loredo, J.; Broome, M.; Hilaire, P.; Gazzano, O.; Sagnes, I.; Lemaitre, A.; Almeida, M.; Senellart, P.; White, A. Boson Sampling with Single-Photon Fock States from a Bright Solid-State Source. *Phys. Rev. Lett.* **2017**, *118*, 130503. [CrossRef]
178. Wang, H.; Qin, J.; Ding, X.; Chen, M.C.; Chen, S.; You, X.; He, Y.M.; Jiang, X.; You, L.; Wang, Z.; et al. Boson Sampling with 20 Input Photons and a 60-Mode Interferometer in a 1E14-Dimensional Hilbert Space. *Phys. Rev. Lett.* **2019**, *123*, 250503. [CrossRef]
179. Lenzini, F.; Haylock, B.; Loredo, J.C.; Abrahão, R.A.; Zakaria, N.A.; Kasture, S.; Sagnes, I.; Lemaitre, A.; Phan, H.; Dao, D.V.; et al. Active demultiplexing of single photons from a solid-state source. *Laser Photonics Rev.* **2017**, *11*, 1600297. [CrossRef]
180. Pittman, T.B.; Franson, J.D. Cyclical quantum memory for photonic qubits. *Phys. Rev. A* **2002**, *66*, 062302. [CrossRef]
181. Lvovsky, A.I.; Sanders, B.C.; Tittel, W. Optical quantum memory. *Nat. Photonics* **2009**, *3*, 706–714. [CrossRef]
182. Saglamyurek, E.; Grimau Puigibert, M.; Zhou, Q.; Giner, L.; Marsili, F.; Verma, V.B.; Woo Nam, S.; Oesterling, L.; Nippa, D.; Oblak, D.; et al. A multiplexed light-matter interface for fibre-based quantum networks. *Nat. Commun.* **2016**, *7*, 11202. [CrossRef]
183. Zhang, W.; Ding, D.S.; Sheng, Y.B.; Zhou, L.; Shi, B.S.; Guo, G.C. Quantum Secure Direct Communication with Quantum Memory. *Phys. Rev. Lett.* **2017**, *118*, 220501. [CrossRef] [PubMed]
184. Bouillard, M.; Boucher, G.; Ferrer Ortas, J.; Pointard, B.; Tualle-Brouri, R. Quantum Storage of Single-Photon and Two-Photon Fock States with an All-Optical Quantum Memory. *Phys. Rev. Lett.* **2019**, *122*, 210501. [CrossRef] [PubMed]
185. Bustard, P.J.; Bonsma-Fisher, K.; Hnatovsky, C.; Grobnic, D.; Mihailov, S.J.; England, D.; Sussman, B.J. Toward a Quantum Memory in a Fiber Cavity Controlled by Intracavity Frequency Translation. *Phys. Rev. Lett.* **2022**, *128*, 120501. [CrossRef] [PubMed]
186. Davidson, O.; Yogev, O.; Poem, E.; Firstenberg, O. Single-Photon Synchronization with a Room-Temperature Atomic Quantum Memory. *Phys. Rev. Lett.* **2023**, *131*, 033601. [CrossRef]
187. Evans, C.J.; Nunn, C.M.; Cheng, S.W.L.; Franson, J.D.; Pittman, T.B. Experimental storage of photonic polarization entanglement in a broadband loop-based quantum memory. *Phys. Rev. A* **2023**, *108*, L050601. [CrossRef]
188. Bustard, P.J.; Tannous, R.; Bonsma-Fisher, K.; Poitras, D.; Hnatovsky, C.; Mihailov, S.J.; England, D.; Sussman, B.J. Toward deterministic sources: Photon generation in a fiber-cavity quantum memory. *Phys. Rev. A* **2024**, *109*, 013711. [CrossRef]
189. Lei, Y.; Kimiaee Asadi, F.; Zhong, T.; Kuzmich, A.; Simon, C.; Hosseini, M. Quantum optical memory for entanglement distribution. *Optica* **2023**, *10*, 1511. [CrossRef]
190. Gerry, C.C. Generation of optical macroscopic quantum superposition states via state reduction with a Mach-Zehnder interferometer containing a Kerr medium. *Phys. Rev. A* **1999**, *59*, 4095–4098. [CrossRef]
191. Zavatta, A.; Viciani, S.; Bellini, M. Quantum-to-Classical Transition with Single-Photon-Added Coherent States of Light. *Science* **2004**, *306*, 660–662. [CrossRef]
192. Zavatta, A.; Viciani, S.; Bellini, M. Single-photon excitation of a coherent state: Catching the elementary step of stimulated light emission. *Phys. Rev. A* **2005**, *72*, 023820. [CrossRef]
193. Zavatta, A.; Parigi, V.; Bellini, M. Experimental nonclassicality of single-photon-added thermal light states. *Phys. Rev. A* **2007**, *75*, 052106. [CrossRef]
194. Parigi, V.; Zavatta, A.; Kim, M.; Bellini, M. Probing Quantum Commutation Rules by Addition and Subtraction of Single Photons to/from a Light Field. *Science* **2007**, *317*, 1890–1893. [CrossRef]
195. Steindl, P.; Snijders, H.; Westra, G.; Hissink, E.; Iakovlev, K.; Polla, S.; Frey, J.; Norman, J.; Gossard, A.; Bowers, J.; et al. Artificial Coherent States of Light by Multiphoton Interference in a Single-Photon Stream. *Phys. Rev. Lett.* **2021**, *126*, 143601. [CrossRef] [PubMed]

196. Biagi, N.; Francesconi, S.; Zavatta, A.; Bellini, M. Photon-by-photon quantum light state engineering. *Prog. Quantum Electron.* **2022**, *84*, 100414. [CrossRef]
197. Akhtar, N.; Wu, J.; Peng, J.X.; Liu, W.M.; Xianlong, G. Sub-Planck structures and sensitivity of the superposed photon-added or photon-subtracted squeezed-vacuum states. *Phys. Rev. A* **2023**, *107*, 052614. [CrossRef]
198. Mendei, B.; Koniorczyk, M.; Homa, G.; Adam, P. Photon Number States via Iterated Photon Addition in a Loop. *Photonics* **2024**, *11*, 1075. [CrossRef]
199. Hong, C.K.; Ou, Z.Y.; Mandel, L. Measurement of subpicosecond time intervals between two photons by interference. *Phys. Rev. Lett.* **1987**, *59*, 2044–2046. [CrossRef]
200. Deng, Y.H.; Wang, H.; Ding, X.; Duan, Z.C.; Qin, J.; Chen, M.C.; He, Y.; He, Y.M.; Li, J.P.; Li, Y.H.; et al. Quantum Interference between Light Sources Separated by 150 Million Kilometers. *Phys. Rev. Lett.* **2019**, *123*, 080401. [CrossRef]